STATE UNIVERSITY OF NEW YORK
AT STONY BROOK

COLLEGE OF
ENGINEERING

Report No. 125

DETERMINATION OF CONCENTRATIONS AND FORMATION ENERGIES AND ENTROPIES OF VACANCY DEFECTS FROM QUENCHING EXPERIMENTS

by

R. W. Balluffi
R. W. Siegel
K. H. Lie
D. N. Seidman

January, 1969

DETERMINATION OF CONCENTRATIONS AND FORMATION ENERGIES AND ENTROPIES OF VACANCY DEFECTS FROM QUENCHING EXPERIMENTS[†]

by

R. W. Balluffi[††]

R. W. Siegel[*]

K. H. Lie[††]

D. N. Seidman[††]

---

† This work was supported by the U. S. Atomic Energy Commission and the National Science Foundation. Additional support was received from the Advanced Research Projects Agency through the use of the technical facilities of the Materials Science Center at Cornell University.

†† Department of Materials Science
Cornell University, Ithaca, New York

* Department of Materials Science
State University of New York at Stony Brook, Stony Brook, L.I., New York

ABSTRACT

A survey is presented of the experimental and analytical techniques available for the determination of concentrations and formation energies and entropies of vacancy defects in pure metals from quenching. Perturbations to the equilibrium population of vacancy defects caused by quenching are considered in relation to their effect upon the quenched-in vacancy defects. The redistribution of vacancy defects as a result of vacancy interactions, the losses of vacancies to existing sinks or by precipitation, and the generation of new defects due to deformation during quenching are examined in detail. Computer calculations have been made for a multi-defect system of vacancy defect clustering and of vacancy losses duirng quenching, and the results are compared with experimental data. Next, experimental methods for the determination of the concentrations of quenched vacancy defects are examined. Indirect techniques which utilize the measurement of a microscopic property such as resistivity or length, for example, in which the change in the property per unit increment of vacancy defects must be known, as well as direct measurements such as electron or field-ion microscopy are discussed. Problems involved in the interpretation of the experimental results from these techniques in terms of defect concentrations such as, non-proportional variation of properties with order of vacancy cluster, non-uniformity of defect distributions and perturbations of the defect population by the observation technique are considered. In addition, measurements sensitive to anisotropic vacancy defect clusters are briefly discussed. Lastly, techniques available for the determination of the formation energies and entropies of single and multiple vacancy defects are considered. Calculations of possible curvature of Arrhenius plots due to both temperature dependence of defect activation energies

and entropies, and to contributions from the various constituents of a multi-defect system have been made, and the results are discussed in the light of possible difficulties which may arise in the interpretation of experimental data. Throughout the discussion of the various topics, available experimental results are considered where pertinent. A number of conclusions have been drawn from the present work and are presented at the ends of the various sections.

Contents

1. Introduction

The population of vacancy defects present in thermal equilibrium may be expressed generally in the form

$$\begin{aligned} c &= c_1 + 2c_2 + \ldots + nc_n \\ &= \alpha_1 \exp(S_1^f/k) \exp(-E_1^f/kT) \\ &\quad + 2\alpha_2 \exp(S_2^f/k) \exp(-E_2^f/kT) \\ &\quad + \ldots + n\alpha_n \exp(S_n^f/k) \exp(-E_n^f/kT) \end{aligned} \tag{1}$$

where n indicates the size of the vacancy cluster, α_n is a constant related to the lattice geometry of the cluster, and S_n^f and E_n^f are the entropy and energy of formation respectively of a cluster of size n which may be functions of temperature. The goal of a quenching experiment aimed at obtaining the equilibrium concentrations and properties of the vacancy defects is to quench the specimen from an elevated temperature, T_q, to a relatively low temperature, rapidly enough to freeze-in the defects present at T_q. Ideally, it is desired to freeze-in the entire equilibrium vacancy defect population in an unperturbed state and, after quenching from various T_q, to measure the c_n individually allowing the absolute determination of the various $S_n^f(T)$ and $E_n^f(T)$.

Unfortunately, this goal cannot be realized in practice, and the purpose of the present work is to examine in some detail the various problems which arise when one attempts to extract quantitative information about vacancy defects from quenching experiments. The problems are taken up in the same order as they occur in quenching experiments. Firstly, it is emphasized in section 2 that real quenches are quite non-ideal, and

that the original equilibrium population present just before quenching is generally significantly altered during the quench. The various perturbing effects are then analyzed and discussed. Secondly, the problems which are encountered in measuring vacancy defect concentrations in specimens after quenching are discussed in section 3. Finally, in section 4, the problems involved in deducing defect energies and entropies of formation from various types of defect concentration data are discussed.

The emphasis in the present work is on the general principles involved, and no attempt is made to present an encyclopedic review of existing experimental results. However, selected data are used wherever possible to illustrate various phenomena. It is unfortunate that in most cases suitable data are available for only one metal; i.e., gold.

In order to simplify the presentation, a list of conclusions is given at the end of each section.

2. Real versus ideal quenches

Inherent perturbing effects which are present in real quenches include:

(1) clustering of the vacancy defect population during the quench.

(2) loss of vacancy defects to sinks such as dislocations during the quench.

(3) generation of additional defects by plastic deformation occurring during the quench.

Let us consider these perturbing effects in detail.

2.1. Clustering of the defect population during quenching

As the crystal is rapidly cooled during the quench, the defects become supersaturated and tend to cluster to at least some degree in cases where positive binding energies exist. This effect is impossible to avoid in reasonably dense systems, since the number of jumps required for a given defect to meet another defect during the quench is generally much smaller than the total number of jumps which the defect could make before being frozen-in during even fast quenches. This effect has been considered by a number of authors, and in order to illustrate the principles involved let us examine the frequently investigated case of the formation of divacancies from monovacancies during the quenching of a fcc metal. Ignoring any defect losses and considering only the redistribution of monovacancies and divacancies, the appropriate approximate equations [1] are

$$\frac{dc_1}{dt} = -168\nu c_1^{\,2} \exp(-E_1^{\,m}/kT) + 28\nu c_2 \exp(-[E_1^{\,m} + E_2^{\,b}]/kT), \qquad (2)$$

$$c_1 + 2c_2 = c = \text{constant}, \tag{3}$$

$$T = T(t), \tag{4}$$

where ν is the atomic vibrational frequency, E_2^b is the divacancy binding energy, and $T(t)$ is the temperature during the quench. Fujiwara [2] was the first to solve the non-linear eq. (2) using computer techniques. He found the following behavior under typical quenching conditions:

(1) At high temperatures where the defects associate and dissociate rapidly, the monovacancy and divacancy populations are able to maintain quasi-equilibrium with each other even in the face of the rapid cooling: i.e., the respective populations follow the relation

$$c_2 = 6c_1^2 \exp(E_2^b/kT). \tag{5}$$

(2) Upon further cooling, a point is reached where the association and dissociation rates become sufficiently sluggish so that the maintenance of quasi-equilibrium is no longer possible. Very soon after that the defects become "frozen-in", and no further changes in their concentrations occur. The freezing-in of the defect distributions occurs rather suddenly near a critical temperature designated as T^*.

We have used a computer to calculate c_1 and c_2 during quenching using eqs. (2) through (4) for a range of conditions and defect parameters which might be typical of a fcc metal, and some results are given in fig. 1 and table 1. As expected (fig. 1), the ratio c_2/c_1 is maintained in quasi-equilibrium during the early part of the quench at elevated temperatures but eventually becomes frozen-in at a constant value at lower temperatures. As seen in table 1, the final value of c_2/c_1 is very sensitive to the values of E_2^b and T_q, and variations of two (or more) orders of

magnitude are possible depending upon the choice of these parameters.

Clustering effects are of little importance for cases where the divacancy binding energy is $\gtrsim$ 0.1eV. Since in many cases the binding energy may be larger than this, we conclude that significant clustering may often occur. Unfortunately, there is a serious lack of any reliable experimental information regarding the properties or the degree of clustering of small vacancy clusters. Of considerable importance is the fact that the degree of clustering is relatively insensitive to the quenching rate. The results show that when the divacancy binding energy is significant it is generally impossible to avoid appreciable clustering even with the use of extremely fast quenches.

As first pointed out by Koehler, et al.[3], an estimate of T* may be obtained by a simple analytical method. The rate at which c_1 must decrease with time in order to maintain quasi-equilibrium during cooling at the rate dT/dt is easily obtained from eqs. (3) and (5) and is given by

$$\left(\frac{dc_1}{dt}\right)^{\circ} = \frac{12c_1^{\,2} \cdot E_2^{\,b} \cdot \exp(E_2^{\,b}/kT)}{kT^2\,[1 + 24c_1 \cdot \exp(E_2^{\,b}/kT)]} \cdot \left(\frac{dT}{dt}\right). \qquad (6)$$

On the other hand, the actual rate at which c_1 decreases as a result of monovacancies meeting to form divacancies is just the first term on the right hand side of eq. (2). In the quasi-equilibrium regime this association term must be large compared with $(dc_1/dt)^{\circ}$. As the temperature drops, however, the association term decreases, and we might expect to obtain an estimate of the freezing-in temperature by setting T* equal to the temperature at which the association term becomes small enough to equal $(dc_1/dt)^{\circ}$.

The result is

$$T^* = \frac{E_2^b \cdot \exp[(E_2^b + E_1^m)/kT^*]}{14\nu \cdot kT^* \sqrt{1 + 48c \cdot \exp(E_2^b/kT^*)}} \cdot \left(\frac{-dT}{dt}\right)_{T = T^*} \qquad (7)$$

Values of T* calculated from eq. (7) are shown by the arrows in fig. 1, and are seen to fall in the middle of the temperature ranges where freezing-in occurs. It is also noted that the quasi-equilibrium ratio at T* is only slightly higher (10-20%) than the actual final frozen-in ratio, and that, therefore, the final ratio may be calculated with fair accuracy from eqs. (7) and (5) without the bother of using the computer.

So far we have considered only the simplest case of monovacancies clustering into divacancies. In general, it is necessary, of course, to consider the possible formation of clusters of all sizes. Cotterill [4] has carried out approximate clustering calculations for a more complicated defect system in which clusters as large as quadri-vacancies were allowed to form. As might be expected, such a system behaves in a manner which is qualitatively similar to the simple monovacancy-divacancy system already described. The various reactions capable of forming the different clusters freeze-in at slightly different temperatures during the quench and eventually all cluster concentrations become completely frozen-in. More details are available in ref. [4].

It is well established that large defect clusters visible by transmission electron microscopy, are formed in many cases when a quenched metal containing a high vacancy supersaturation is annealed at a low temperature. The following question therefore arises. Is it possible to quench at a sufficient rate to restrict the clustering during the quench

to the formation of small mobile clusters, or are larger more immobile clusters formed which are capable of growing into large visible clusters during low temperature annealing? Meshii, et al. [5] have shown that the formation of larger visible clusters in quenched gold and aluminium requires nucleation, and they have demonstrated that the nucleation occurs only below a critical temperature (~160°C in gold). Furthermore, by quenching at reasonably rapid rates they were able to avoid completely the formation of any nuclei for the large visible clusters. These results indicate that the formation of relatively large immobile clusters may be generally avoided in quenching experiments.

As shown above, it is impossible to avoid clustering in systems where the clusters possess significant binding energies even when extremely fast quenches are used. If we assume that the c_n can be measured individually after quenching to T_o it is obvious that the c_n which are measured experimentally will be those in quasi-equilibrium at T* rather than the desired concentrations in true thermal equilibrium at T_q. It might be thought that in this situation the c_n could be measured as functions of quenching rate after quenching from a fixed T_q, and that the desired values of c_n corresponding to thermal equilibrium at T_q could then be obtained by extrapolating the results to an infinite quenching rate. However, inspection of the results in fig. 1 shows that such an extrapolation would be very long and uncertain and would therefore be quite unreliable. This is more clearly shown in fig. 2 where the nature of the extrapolation may be seen for a specific case. Since 10^5°C · sec^{-1} is about the upper limit of presently available quenching rates, it appears that there is no quenching method currently available which will allow the reliable determination of the true thermal equilibrium values of the c_n.

Conclusions:

(1) At least some degree of clustering in the form of small mobile clusters occurs during usual quenching in systems where the clusters possess significant binding energies. The results are relatively insensitive to the quenching rate. The extent of such clustering naturally depends directly upon the properties of the small clusters. Unfortunately, there is a serious lack of any reliable information regarding either the properties or the degree of clustering of these defects.

(2) Cluster concentrations become frozen-in rather abruptly at some critical temperature during quenching.

(3) The formation of relatively large immobile clusters may be generally avoided during quenching.

(4) Even if the concentrations of the individual clusters could be measured individually after quenching as a function of quenching rate, attempts to extrapolate the results to an infinite quenching rate in order to obtain the individual cluster concentrations originally present in thermal equilibrium at T_q would most likely fail.

2.2. Vacancy losses during quenching

In specimens quenched at finite rates a certain fraction of the supersaturated vacancies is inevitably lost at sinks which are present in the specimen during the quench. Possible sinks include the free surface, grain boundaries, subgrain boundaries (dense planar arrays of dislocations), and the random 3-dimensional dislocation network. As pointed out below in section 2.3, dislocations may be generated in plastic deformation during quenching, and, therefore, the possible sinks include those present in the specimen just before the quench as well as those generated during the quench. It is also possible under special circumstances (i.e., slow quenches, or cases where sinks are absent †) for the supersaturated defects to build up larger clusters during the quench so that large immobile vacancy precipitates (i.e., dislocation loops, voids, stacking-fault tetrahedra, etc.) form which in turn act as vacancy sinks during their growth. We regard this possibility as a special case, however, and shall not consider it further. The relative importance of the sinks mentioned above depends, of course, upon their relative densities and the efficiency with which they absorb vacancy defects.

In recent years there has been an increasing awareness that vacancy losses during quenching play an important role in quenching experiments, and a number of workers have quenched at different rates in order to evaluate the losses as a function of quenching rates. Flynn, et al. [7], in one of the most complete studies, obtained the results shown in fig. 3

---

† For example (see ref. [6]), large vacancy precipitates have been formed by clustering in single crystals of almost dislocation - free copper during furnace cooling (quenching?).

for the case of gold. The data show a total defect resistivity (concentration) loss which increases as the quenching rate is decreased or the quenching temperature is increased. At sufficiently low quenching temperatures essentially all losses were avoided by quenching at moderately fast rates. For any given elevated quenching temperature the data may presumably be corrected for quenching losses (and the thermal equilibrium defect resistivity (concentration) may be deduced) by extrapolating the quenched-in resistivity increment to infinite quenching rate as shown in fig. 4. Comparison of figs. 4 and 2 shows that the technique of extrapolating to infinite quenching rate as a means of correcting for losses due to finite quenching rates is considerably more reliable for correcting for losses than for clustering. Loss data showing the same general features have been obtained in other investigations with gold [8-10], platinum [11] and aluminium [12], and also in work in progress on bcc metals by Bass and coworkers [13].

The general features of this behavior are readily understood in terms of the relative numbers of the supersaturated defects which are able to reach the sinks by diffusion during the quench. However, the attainment of a detailed quantitative understanding of the results is considerably more difficult. The simplest model which can be visualized is one in which only one vacancy type defect is present, and where the specimen contains a constant density of fixed sinks during the quench which operate with a sufficiently high efficiency to maintain the point defect concentration in their direct vicinity at the instantaneous equilibrium concentration called for by the specimen temperature. Under these conditions the defect loss is controlled by the amount of defect diffusion which can take place to the sinks during the quench in the

presence of the continuously varying equilibrium boundary condition at the surfaces of the sinks. Flynn, et al.[7] showed that a reasonably accurate approximate solution to this problem could be obtained in the form of an eigenfunction expansion, and, furthermore, showed that for linear quenches the fractional loss of the total vacancy concentration to fixed sinks is a function which depends only on the combined parameter $D_q T_q \tau_q$ where D_q is the defect diffusivity at T_q and τ_q is the time required for the quench. However, in order to calculate actual losses for given types of sinks it is necessary to carry out detailed calculations utilizing the appropriate eigenfunctions. In the present work we have avoided these complications and have calculated defect losses in a typical quenched system by direct numerical integration of the defect diffusion equation in the presence of an appropriate temperature (time) dependent diffusivity and equilibrium temperature (time) dependent boundary conditions at the sinks.

The dominant sinks are expected to be dislocations, and to a lesser degree, subgrain boundaries. It has been shown elsewhere [14] that typical planar sub-boundaries consisting of dislocations which act as high efficiency sinks should act as perfect planar sinks. Since the subgrain size is generally smaller than the grain size (or specimen size), we may regard the subgrains as the most important planar type sinks and therefore we need only consider the sub-boundaries and dislocations in our calculations. Unfortunately, it has not been practicable to calculate the losses due to the simultaneous presence of both dislocations and subgrain boundaries. We have therefore calculated losses to each of these sink types separately on the assumption that it alone is operative. This

procedure, of course, tends to overestimate the loss which would occur at each sink type in the actual combined case. Idealized models for calculating the diffusion to each type of sink were employed. The dislocation structure was represented by an array of straight parallel dislocations each surrounded by a cylindrical diffusion cell of radius $(\pi N_d)^{-1/2}$ where N_d is the dislocation density, while the subgrains were represented by spheres of radius R. Extensive discussions of these idealized models have been given elsewhere [7,10,14-16]. Dislocation densities and subgrain radii in quenched gold have been measured [16,17] and are of order $\sim 5 \times 10^7$ cm^{-2} and 60-200μ respectively. Some results for a simple assumed monovacancy system containing sinks at the above densities are given in figs. 5 and 6.† It is seen in Fig. 6 that the dislocations are the dominant sinks under these conditions.

The calculated results (figs. 5 and 6) show behavior which is at least qualitatively similar to the experimental results (figs. 3 and 4). Such idealized calculations therefore are capable of offering at least a good semi-quantitative explanation of defect losses during quenching. However, the following simplifying assumptions have been made which require further discussion:

(1) the dislocations act as perfect line sinks during the entire quench.

(2) the dislocation density is constant during the quench.

(3) only one defect type is present, and clusters (and clustering) are neglected.

† We have verified that fractional losses in fig. 5 are a unique function of $(D_q T_q \tau_q)$ as predicted by Flynn, et al. [7]

(4) an idealized fixed sink structure is an acceptable approximation.

The situation with respect to the efficiency of the dislocation network as line sinks for supersaturated vacancies has been extensively reviewed by Balluffi and Seidman in several papers [10,15,16,18]. The general conclusion is that the network climbs with a relatively high efficiency (i.e., a rate which is within a factor of 1/10 to 1 of the maximum possible diffusion limited rate) under conditions of moderate to strong defect supersaturation. There is some evidence, summarized in a recent paper by Wang, et al. [10], that the sink efficiency, in gold at least, is somewhat reduced when the vacancy supersaturation (i.e., the driving force for climb) is in the range corresponding to a vacancy chemical potential $\gtrsim$ 0.1eV. This would suggest that the defect losses during the early part of the quench during the period of relatively low supersaturation might be lower than calculated above on the assumption of perfect sinks. We note that Kino and Koehler [9] have suggested that line tension may play a significant role in controlling the dislocation sink action during quenching when dislocation segments must bow out in order to climb. They argue that the network is then inoperative during the initial period of the quench until enough vacancy supersaturation ($\simeq$1%) is built up to provide the driving force required to bow out the segments. However, if the network is initially annealed it is unlikely that significant amounts of bowing are necessary for climb during the early stages of the quench during which the supersaturation is building up to only $\sim$1%. Furthermore, even if the dislocations were inoperative during this period the overall effect on the losses would be exceedingly

small.† We conclude that dislocation line tension effects may be ignored in a consideration of the loss problem.

The assumption that the dislocation density is constant is undoubtedly a poor approximation in most cases since, as discussed in section 2.3, there is considerable evidence that significant dislocation generation and movement occurs under many quenching conditions. Losses could be enhanced considerably in such cases due to the sweeping up effect of the moving dislocations.

In systems with significantly high cluster binding energies the cluster diffusion to sinks could be important, and would have to be considered in calculating the losses. Flynn [19], for example, has indicated some analytical techniques which might be useful in coping with this problem. So far, no extensive calculations of losses in the presence of clustering have been made.

The effects of non-uniformly distributed dislocations on annealing kinetics have been investigated by Ham [20], and the effects of non-uniformly shaped subgrain boundaries have been discussed by Flynn, et al. [7].

† Kino and Koehler [9] also suggest that significant nucleation of vacancy precipitates could occur during the short initial period during which the dislocations are assumed to be inoperative. However, since any vacancy concentration decrease during this period would be relatively small such processes would proceed independently of the rapidity of the sink action at the dislocations. It should also be pointed out that much larger supersaturations are required to nucleate vacancy precipitates than bow out dislocations, and that the critical temperature for vacancy precipitate nucleation in quenched gold is about 160°C.

The general conclusion is that the idealized models described above should be reasonably good approximations under usual conditions.

In view of the difficulties mentioned above we have not attempted to obtain a close quantitative fit of the idealized loss model to existing data. In the case of gold, for example, there is the added difficulty of current uncertainty with respect to the properties of monovacancies and divacancies [10,21]. It should also be emphasized that there is only one case [17] (i.e., the case of gold) in which dislocation densities have been measured directly in quenched metals. Values in the range of $\sim 5 \times 10^{7}$ cm^{-2} were found. Further measurements of this quantity would be of great interest.

As a final topic we would like to discuss the accuracy with which quenching data can be corrected for losses by quenching at different rates and then extrapolating the results to an infinite quenching rate as in fig. 4. This technique, which has been criticized recently by Seeger and Mehrer [22], is of great importance, since it is potentially the only way in which the effect of losses may be eliminated by a direct method. The technique has been criticized on the basis that the results are perturbed by specimen deformation which increases with the quenching rate. However, as Jackson [23] has shown (see section 2.3), the effects of deformation induced defects are generally to reduce quenched-in defect concentrations rather than enhance them, since the sink effect of strain induced dislocations is more important than the production of new defects by the deformation. If experiments show increments which increase with increased quenching rate and approach a finite limit at the limit of an infinite quenching rate, then it is reasonable to suppose that the decreased time available for the diffusional loss to sinks more than

compensates for the effects of any increase in the dislocation sink density. Since this is found to be generally the case [7-12], we conclude that the true equilibrium increment with no losses is obtained at the limit of infinite quenching rate. In this respect it is of interest to examine the results of a number of experiments of this type which have been performed on gold presented in fig. 7. The high temperature points of Simmons and Balluffi [24] were obtained from measurements of specimen length and x-ray lattice parameter changes under equilibrium conditions and represent values of the total absolute concentration of vacant lattice sites. The remaining data, with the exception of the low temperature data point of Bass [25], were obtained from electrical resistivity quenching experiments where the quenched-in increments were obtained by extrapolations to infinite quenching rates. The corresponding concentrations were calculated from these data using 1.5×10^{-6} Ω cm as the resistivity of 1 at. % of vacant sites. This value is seen to produce a smooth grafting together of the high temperature absolute measurements of Simmons and Balluffi and the remaining resistivity based data. Wherever necessary the data were converted to a common temperature scale corresponding to the resistance versus temperature data of Meechan and Eggleston [26]. All data were also normalized to agree with the value of 2.25×10^{-6} Ω cm for the resistivity of gold at 25°C from ref. [25]. The data are all seen to fall remarkably well on a single curve. The mean absolute percentage deviation of the 18 data points, all obtained by the extrapolation technique, was 4.4%. The relatively good agreement of the data obtained in these different investigations support the conclusion that this extrapolation technique is a reliable method for obtaining equilibrium concentrations from quenching experiments.

Conclusions:

(1) Appreciable vacancy defect losses, primarily to dislocations and to a lesser extent to subgrain boundaries, generally occur in specimens quenched from elevated temperatures.

(2) A relatively simple model based upon defect diffusion limited losses to existing dislocations (and subgrain boundaries) is capable of explaining the main features of existing loss data.

(3) Exact and reliable calculations of losses are complicated by: (a) a lack of precise knowledge regarding the sink efficiency of dislocations; (b) possible increases in the dislocation sink density during the quench; and (c) a lack of knowledge of the degree of defect clustering during the quench and the effect of such clustering on the losses.

(4) The method of correcting for defect losses during quenching by quenching at different rates and extrapolating the quenched-in increment to infinite rate in order to obtain equilibrium concentrations is a legitimate technique.

2.3. Effects of quenching strains

A rapidly quenched specimen is always at least slightly strained during rapid quenching because of: (1) the internal stress, due to differential thermal contraction, which is present when the outside of the specimen is cooled relative to the interior; (2) the applied stress due to the hydrodynamic drag which is exerted on the specimen if it is plunged into a liquid quenching medium†. Plastic straining by these means may affect quenching results in two ways: (1) the straining produces unwanted extra point defects and dislocations; and (2) the extra dislocations act as sinks for both the original equilibrium vacancy population and any point defects generated during the quench. The a priori effect of plastic straining may, therefore, be to either increase or decrease the defect concentration obtained after quenching relative to the equilibrium concentration depending upon the relative magnitudes of the two effects described above.

The various possibilities have been investigated extensively by Jackson [23] both theoretically and experimentally. Jackson calculated the maximum plastic shear strains in gold-wires due to internal thermal stresses after linear quenching into water, and the results are shown in table 2. He also calculated the hydrodynamic stretching strains in initially straight gold wires after fast quenching into water (see table 3). The results show that the thermally generated strains increase with increased wire diameter, whereas the hydrodynamically induced strains

† This latter effect is, of course, absent in specimens which are gas-quenched in still gases.

behave in the opposite manner. Furthermore, the thermally generated strains are very small (of the order of 10^{-5}) for specimens with diameters similar to those usually employed in quenching experiments (i.e., <0.041 cm). On the other hand, the hydrodynamic strains may become as large as 3×10^{-3} for wires of diameter near 0.005 cm. Jackson [23] presents extensive experimental evidence which indicates that the calculated quenching strains in tables 2 and 3 are of the correct order of magnitude.

We must now consider the point defect and dislocation effects which may be expected from the quenching strains indicated above. If it is assumed for purposes of making preliminary order-of-magnitude estimates that the point defect production and dislocation generation in plastic deformation are <u>independent</u> of temperature, then we may estimate from experiments at, or below, room temperature that $\sim 10^{-7}$ atom fraction point defects are generated in gold by a strain of 10^{-3} (see refs. [27,28]). This concentration is equal to the concentration of vacancies in thermal equilibrium at about 375°C (i.e., $T(°K)/T_m(°K) = 0.48$ where T_m is the melting temperature). Since 375°C is an unusually low quenching temperature for gold, we may conclude that the point defect concentration induced by quenching strains would be of minor importance under all conditions except in thin specimens liquid-quenched from very low quenching temperatures.

An upper limit of the dislocation density generated in gold by a quenching strain of 10^{-3} may also be estimated from low temperature data giving resistance increases due to deformation [27,28] and the specific resistivity of dislocations [29]. The result is about 4×10^{7} dislocations

cm^{-2}. (This is an upper limit, of course, since dislocation annealing would undoubtedly occur at elevated quenching temperatures.) In the case of resistivity quenching experiments the resistance of the above dislocations would be about the same as that of the strain generated point defects and would therefore again be of little importance except in thin specimens liquid-quenched from very low quenching temperatures.

The effect of strain generated dislocations as sinks for vacancy defects during quenching is much more difficult to estimate. If we assume that the strain generated dislocations are present during the entire quench and act as stationary perfect line sinks for supersaturated vacancies during the quench, then it is readily shown, using the methods employed in section 2.2, that a dislocation density of 4×10^7 cm^{-2} could absorb a significant fraction of the vacancies which were present just before the quench. It must be emphasized, however, that these assumptions are highly oversimplified. The continuous production and thermal annealing of the strain induced dislocations at the elevated temperatures would tend to decrease the average density below that estimated above. However, the newly generated dislocations would sweep through the sea of supersaturated vacancies, and would, therefore, absorb more vacancies than a stationary array of dislocations. Without attempting any detailed calculations of this complex problem we may conclude that for sufficiently high quenching temperatures it seems highly likely that a significant fraction of vacancies may be absorbed at dislocations generated by strains during quenching.

Jackson [23] has carried out a series of decisive experiments which are consistent with the previous discussion. He quenched 0.041 cm dia

platinum wires at a rate of $5.5 \times 10^4 °C \cdot sec^{-1}$ under conditions where the specimen could be strained a predetermined amount by an externally applied force during the quench. The point defect resistance increment after quenching when strain was applied, $\Delta R(\varepsilon)$, was then compared to the increment obtained after a similar quench in the absence of strain, $\Delta R(0)$. The results are shown in table 4. It is seen that significant fractions of the vacancy concentrations were absorbed at dislocations generated by strains greater than 10^{-3} during quenches from the highest temperature. The sink action of the dislocations generated by the straining during the quenching more than compensated for the number of excess point defects generated by the straining. Jackson also concluded that the concentration of vacancies produced by unit strain in platinum is much the same at all temperatures between 78°K and elevated quenching temperatures. We note that these conclusions are consistent with the demonstration by Ruoff and Balluffi [30] that the large so-called strain enhanced bulk diffusion effects reported by many authors in the past must have been due to experimental errors, or in some cases, to short circuiting along dislocations.

Effects of quenching strains generally consistent with the above discussion are apparent in a large number of quenching experiments. For example, Ascoli, et al. [31] found evidence for strain induced defects in water quenched 0.0041 cm dia platinum wires. More recently Kino and Koehler [9] quenched 0.016 cm thick gold ribbons into water and found a small excess resistivity increment after quenching from very low temperatures which was most likely due to strain-induced defects. The only work in disagreement with the present point of view is that of Takamura [32]

who claimed evidence for the production of huge numbers of vacancies by quenching strains in water quenched gold rods with diameters in the range of 0.10 to 0.30 cm. This investigator claimed that the number of vacancies produced by quench strains was of the same order of magnitude as the equilibrium number of vacancies after quenches from temperatures as high as 850°C. These results are seen to be in direct contradiction to the conclusions of Jackson [23]. Moreover, more recent quenching experiments by Fraikor and Hirth [33] using specimens similar to those of Takamura have failed to reproduce the Takamura results, and instead are consistent with Jackson's work and the present point of view. We may therefore argue that the Takamura results should not be taken as evidence against the present conclusions.

Conclusions:

(1) Thermally induced quenching strains during the water quenching of normal specimens (dia<0.041 cm) are small, i.e., $<10^{-5}$.

(2) Hydrodynamic stretching strains during the water quenching of normal specimens are larger, i.e., $\sim 8 \times 10^{-4}$ for dia = 0.041 cm and $\sim 34 \times 10^{-4}$ for dia = 0.005 cm.

(3) The number of vacancies generated by quenching strains is expected to be small relative to the number quenched-in except for the case of thin specimens liquid quenched from very low quenching temperatures.

(4) Quenching strains of the order of 10^{-3} may be expected to generate enough dislocations to absorb a significant fraction of the vacancies initially present at elevated quenching temperatures.

(5) At elevated temperatures quenching strains cause a net loss of vacancies, since the sink effect of the dislocations which are generated more than compensates for the extra defects produced by the deformation.

3. Measurements of vacancy defect concentrations

Having considered the inherent perturbations to the high temperature equilibrium vacancy population caused by quenching, we now consider the problem of measuring the concentrations of the vacancy defects which have been quenched into a pure metal. Ideally one would like to be able to measure directly the individual concentrations of the various vacancy clusters, c_n, which are present after quenching. However, as pointed out below, only approximate values of the total quenched-in concentration of vacant lattice-sites, c, have been made to date.

3.1. Direct determination of the individual concentrations of vacancy clusters, c_n

The only presently available technique for a direct determination of the various c_n is field ion microscopy (FIM). This technique could, in principle, give a measure of the partition between monovacancies, divacancies and higher order clusters present after a quench. An absolute measurement of the c_n by FIM would in addition yield the binding energy of the various clusters. As an example, consider a system consisting of only monovacancies and divacancies as in fig. 1. If this system were quenched from 700°C the observed ratio c_2/c_1 would be determined by the divacancy binding energy (see fig. 1). Hence, it should be possible to distinguish between a low binding energy (0.1 eV) where divacancies would be essentially nonexistent (∿1 out of every 1,000 defects would be a divacancy) and a high binding energy (0.4 eV) where ∿1 out of

every 5 defects would be a divacancy.† We now proceed to examine some of the complications associated with the use of FIM for the direct determination of c_n.

The most significant problems involved in the determination of c_n by FIM are: (1) the presence of artifact defects; (2) stress induced defect migration caused by the electric field on the specimen which would tend to reduce the concentration of defects; and (3) the sampling problems associated with observing a statistically significant defect concentration.

Possible sources [34] of artifact defects are:

(i) defects formed as the result of field evaporation performed in a helium-neon gas mixture [35];

(ii) field induced chemical etching in the presence of water vapor in the case of tungsten and platinum [36];

(iii) preferential field evaporation of solute atoms in dilute alloys;

(iv) a lowering of the free energy of formation of a monovacancy due to the tensile stress produced by the high electric field at the surface of a specimen tip.

The first two sources of artifact defects listed here do not present a serious problem since they may be controlled by the experimentalist. The third item is also not a serious handicap if the investigations are restricted to high purity ($\gtrsim$99.9999 wt. %) specimens. The most serious possible cause of artifact defects is (iv) which we shall consider in some

---

† We have assumed a quenching rate of between 10^4 and 10^5°C sec^{-1} for this illustrative example.

detail. We first consider the possibility that the electric field on the tip provides a high enough tensile stress to induce significant bulk defect concentrations. Then we consider the possibility that significant numbers of defects can be generated on the stressed crystal surface planes.

The bulk equilibrium monovacancy concentration as a function of pressure, p, and temperature is, of course, given by

$$c_1 (p,T) = \exp(-\Delta G_1^f/kT), \tag{8}$$

where ΔG_1^f is the Gibbs free energy of formation. Equation (8) may also be expressed in the form

$$c_1 (p,T) = c_1(p_o,T) \exp\left[\frac{\Delta V_1^f |(p - p_o)|}{kT}\right], \tag{9}$$

where ΔV_1^f is the volume of formation of a monovacancy, p_o is the gas pressure in the FIM, and p is the pressure on the surface of the tip due to the electric field. It has often been assumed [37] that a semi-reasonable model for the specimen tip is a sphere of radius r, so that the tension, $|(p - p_o)|$, acting on the surface is given by $\varepsilon\varepsilon_o E^2/2$ (in mks units) [38] where E is the electric field (volts·m^{-1}) at the surface of the tip. Hence, the effect of the field is to increase the bulk monovacancy concentration relative to its equilibrium value at p_o and T. The quantity of concern then is the value of $c_1(p,T)$ at the imaging temperature. It is not sufficient to compare only roughly the size of E_1^f relative

to $\Delta V_1^f|(p - p_o)|$, since at the typical imaging temperatures used in field ion microscopy the value of kT is quite small. For example, even if the quantity $[E_1^f - \Delta V_1^f|(p - p_o)|]$, i.e., the effective formation energy, were as small as 0.1 eV the induced monovacancy concentration at 20°K would only be $\sim 6 \times 10^{-25}$. Hence, a more suitable criterion for the lack of field induced vacancies, within the context of the above model, would more realistically be the condition that $c_1(p,T) < 10^{-6}$.

The above simple spherical model for the specimen tip is however not physically realistic, since one should actually solve for the three dimensional stress distribution in a non-spherical tip subjected to a set of surface tractions which varies something like that illustrated schematically in fig. 8. This is a rather difficult analytic problem because of the variable boundary condition on the tip surface, and, hence, the exact stress distribution within the tip is presently unknown. However, one can obtain an estimate of how the surface tension falls off with distance from the surface by analogy to the problem of a cone subjected to a point load [39]. For the latter problem, neglecting the angular dependence, all of the stresses fall off as $1/r^2$. Hence, one would expect that the state of stress at and near the surface would be very important with respect to the lowering of the free energy of formation of a vacancy.

Schwoebel [40] has recently used a nearest neighbor binding model to calculate the energy of formation of a monovacancy, $[(E_1^f)_{hkl}]$, on various crystallographic surface planes of fcc crystals.† The general result he finds is that, as the coordination number of an atom on a given plane

† Further calculations by Beeler, presented in this conference, for a bcc crystal show the same general characteristics.

decreases, the monovacancy concentration increases. The calculations which Schwoebel made were for unstressed crystal surface planes, while we are interested in the vacancy concentration on a crystal surface plane (hkl) in the stressed state. The effective formation energy for a monovacancy on an (hkl) surface plane in the stressed state is

$$[(E_1^f)_{hkl} - (\Delta V_1^f)_{hkl} |(p - p_o)|_{hkl}] , \qquad (10)$$

where $(\Delta V_1^f)_{hkl}$ is the volume of formation of a vacancy on the (hkl) plane, and $|(p - p_o)|_{hkl}$ is the tensile stress acting on (hkl). Unfortunately this quantity is rather difficult to evaluate at present, but it is conceivable that it could be a good deal smaller than $[E_1^f - \Delta V_1^f |(p - p_o)|]$, so that $c_1[p,T, (hkl)]$ might become significant at even the rather low FIM imaging temperatures.

The second effect of the stress produced by the evaporation or imaging electric field is to increase the diffusivity of vacancies and to therefore cause a stress induced migration which could lower the observed value of c_n. For monovacancies the diffusion coefficient is given by

$$D_1 = a^2 \nu \exp[-\Delta G_1^m/kT] , \qquad (11)$$

where a is the lattice parameter, and ΔG_1^m is the Gibbs free energy of migration. Following procedures similar to those employed in obtaining eq. (9) from eq. (8) it can be shown that

$$D_1(p,T) = D_1(p_o,T) \exp[(\tfrac{2}{3} - \gamma)\cdot\chi\cdot|(p - p_o)|] \exp[\frac{\Delta V_1^m}{kT}|(p - p_o)|], \qquad (12)$$

where γ is the Grüneisen constant, χ is the expandability, and ΔV_l^m is the volume of migration of a monovacancy.† Since $\Delta V_l^m|(p - p_o)|$ is positive, the field will cause a monovacancy to anneal at an apparently lower temperature than it would in the absence of the field. Let us now consider the magnitude of this effect. In table 5 we present the results of a calculation of the monovacancy diffusion coefficient in platinum in the stressed and unstressed state, where a value of $\Delta V_l^m = 0.2$ atomic volume was assumed.†† It is seen (for this value of ΔV_l^m) that the diffusion coefficient in the stressed state is not large enough to produce an observable effect as long as the specimen is stressed at or below 78°K. Physically what is required is that the value of the diffusion coefficient in the stressed state be small enough so that the root mean square diffusion distance $\left(\sqrt{\bar{x}^2} = \sqrt{2D_l t}\right)$ is less than one lattice spacing, so that even subsurface vacancies are not caused to diffuse out of the specimen by the electric field. This is seen to be the case for the illustrative calculation of monovacancies in platinum at temperatures less than ~78°K.

† The quantities a, ν and ΔG_l^m were all considered to be pressure dependent in the derivation of equation (12). We have assumed that the lattice frequency obeys the Grüneisen relationship, that γ and χ are temperature independent, and that the lattice expandability is the negative of the lattice compressibility.

†† The only measurement of ΔV_l^m has been made by Emrick [41] by measuring the pressure dependence of the annealing rate of defects (monovacancies or divacancies?) in quenched gold. He obtained a value of 0.15 atomic volume for ΔV_l^m.

The sampling problem in FIM is a result of the fact that the vacancy defect concentrations in quenched metals are quite small. A reasonable quenched-in vacancy defect concentration for a rapid quench from near the melting point of platinum is $\sim 2 \times 10^{-4}$. Hence, one would have to examine at least 5,000 atom sites in order to find only 1 defect. Thus the experimentalist must be prepared to field evaporate through many atomic net planes in his search for vacancy defects. A statistically significant number of defects would be ~100 for a c_n determination, which implies examining 5×10^5 atom sites on high index net planes where each atom is fully resolved. A main difficulty with examining these 5×10^5 atom sites is that the atomic resolution is a function of the size of the plane. An excellent example of this phenomenon has been given by Brenner [42] who dissected the (332) plane of tungsten one atom at a time and resolved a monovacancy only when the number of lattice sites on this plane had been reduced to 15. Therefore an accurate determination of c_n would require on the order of 5×10^5 frames of film because of the necessity for careful incremental field evaporation of atomic net planes. This problem obviously requires some automation of the pulse field evaporation amplifier and camera recording system.† An example of the atom by atom dissection of the (334) plane of tungsten, using the data recording system in our laboratory at Cornell, is shown in fig. 9. A quantity as large as 5×10^5 frames of film is by no means prohibitive†† by modern technological

† At Cornell University [43] we have constructed an external image intensification and data recording system for a field ion microscope with exactly the above problem in mind.

†† The quantity 5×10^5 frames of film represents approximately 335 rolls of 100-foot film spools.

standards, and in addition, many of the techniques of scanning film have already been solved by high energy nuclear physicists [44].

The experimental applications of the FIM to the problem of absolute determinations of c_n have been rather sparse. The first application of the FIM to this problem was made by Müller [45]. He quenched a platinum specimen from near the melting point, then prepared an FIM tip of this specimen and subsequently field evaporated through 71 successive (201) planes to find 5 vacant lattice sites among the 8,500 atoms inspected. This small number of observations is clearly not statistically significant, but the experiment illustrates the feasibility of this type of investigation. A more recent experiment on the same problem has been conducted by Speicher, et al.[46]. They focussed their attention on unquenched well-annealed platinum specimens and found monovacancy concentrations as high as 7.5×10^{-3} on the (012) plane at 21°K. They attributed this to bulk stress induced monovacancies associated with the field evaporation process. These concentrations are considerably too high to be induced by bulk stresses. It is relatively easy to show† that an evaporation field of ∿21 volts · $\mathring{A}^{-1}$ would be required to induce a bulk concentration of 7.5×10^{-3} at 21°K. We therefore tentatively suggest that the anomalously high vacancy concentrations on the (012) plane may have been the result of an exceedingly low value of $[(E_1^f)_{hkl} - (\Delta V_1^f)_{hkl} |(p - p_o)|_{hkl}]$.

---

† The expression for the equilibrium concentration of monovacancies was taken to be $\exp(1.5) \cdot \exp(-1.5\text{eV}/kT)$ from the work of Jackson [11], and a value of 0.5 atomic volume was used for ΔV_1^f. The value of $|(p - p_o)|$ necessary to satisfy eq. (9) for a concentration of 7.5×10^{-3} at 21°K is 2×10^{12} dyne cm^{-2}.

As part of a general program on vacancy defects in gold we are employing the FIM as a research instrument and have succeeded in obtaining well developed, stable end forms of gold [47]. An example of a gold specimen imaged with a 25% Ne-He gas mixture at ~16°K is shown in fig. 10. At present, detailed experiments are in progress on the imaging characteristics of gold specimens and a number of controversial questions concerning vacancy defects in gold.

In conclusion, it is emphasized that the field ion microscope has a very strong potential for solving a number of outstanding problems concerning vacancy defects, but that there are associated problems with respect to artifact vacancies, data recording, and data reduction that must also be simultaneously solved if this potential is to be realized.

3.2. Direct determination of the total concentration of vacant sites, c

Although field ion microscopy offers the only presently available method for determining the individual c_n values, two other techniques can be used to find the total concentration of quenched-in vacant sites, c, directly: i.e., transmission electron microscopy and simultaneous measurements of length and lattice parameter changes. The use of electron microscopy to determine c requires that all of the quenched-in vacancy defects precipitate into observable, and recognizable defect clusters. Under this condition, and if the relationship between the precipitate size and the number of vacant sites stored in the precipitate is known, the total quenched-in vacant site concentration can be directly determined. Cotterill [48] was the first to use this technique for concentration determinations over a range of

quenching temperatures. His results were in poor agreement with the measured equilibrium concentrations for gold [24], but this was probably a result of sampling difficulties. Considerable care in statistical sampling must be taken if this technique is to be used successfully. Regions (e.g., near grain boundaries) in which significant defect losses have occured during either quenching or subsequent low temperature annealing must be avoided. In addition, perturbations of the defect structure caused by the thin film techniques (e.g., dislocation loop loss from thin foils) must be avoided or taken into account [49]. The problem of having a detailed knowledge of the relationship between the size of the vacancy precipitates and the number of vacant sites stored may be considerable. In cases where the precipitate structure is incompletely understood, as in the case of "black-spot defects" [50], evaluation of the total site concentration by this technique may prove inaccurate.

Another direct technique for the determination of the total quenched-in concentration, which somewhat surprisingly has never been performed on quenched metals, is the simultaneous measurement of length and lattice parameter changes. These measurements, which have provided our most unambiguous knowledge of the total vacant site concentrations in metals under thermal equilibrium conditions, are well suited to concentration determinations in quenched metals. If f is the fractional atomic volume relaxation around a vacancy, then the fractional length change upon the addition of a concentration c of vacant sites (assuming isotropic dilatation) is given by

$$\frac{\Delta L}{L} = \frac{1}{3} c(1 - f), \qquad (13)$$

and the fractional lattice parameter change is given by

$$\frac{\Delta a}{a} = -\frac{1}{3} cf. \qquad (14)$$

Subtracting (14) from (13), we obtain the well known relation

$$c = 3\left(\frac{\Delta L}{L} - \frac{\Delta a}{a}\right). \qquad (15)$$

If a specimen is quenched and then annealed at temperatures at which the vacancy defects anneal only at pre-existing sinks such as dislocations, grainboundaries and surfaces, with measurements of ΔL and Δa being made in the as-quenched condition, at intermediate points, and in the fully annealed state, then the total vacant site concentration present in the material may be directly determined by eq. (15). A graphic representation of this type of measurement is shown in fig.11 where a value of $f = \frac{1}{4}$ is assumed, and the curves for $\frac{3\Delta L}{L}$ and $\frac{3\Delta a}{a}$ have been plotted together so that their asymptotes in the fully annealed state superimpose. The difference between the two curves is always equal to the absolute value of c in the metal.

3.3. Indirect determination of the total concentration of vacant sites, c

Most of the experimental investigations of defect concentrations in quenched metals have utilized indirect techniques in which a measurement of the total change in some macroscopic property, Δp, caused by quenching is made, and this change is then related to the concentration of vacancy defects through a knowledge of the property change per defect. In general

$$\Delta p = \sum_n p_n c_n \ , \tag{16}$$

where p_n is the change in p due to unit concentration of vacancy clusters of size n. If we define an average value, A, for the change in p due to unit concentration of individual vacant lattice sites (i.e., averaged over all cluster sizes) then

$$\Delta p = \left[\frac{\sum_n p_n c_n}{\sum_n n c_n}\right] \cdot c = A \cdot c \ . \tag{17}$$

If the p_n vary linearly with n (i.e., $p_n = np_1$) then $A = p_1$. Equations (16) and (17) show that c is only strictly proportional to Δp when either no clustering is present or the p_n vary linearly with n. Possible effects due to non-linearity have been customarily ignored in quenching experiments and eq. (17) has, therefore, been employed, with the tacit assumption that A is independent of c, as an approximation to obtain c. The quantitative nature of this approximation may be illustrated by using the simple monovacancy-divacancy model which was used previously to calculate the clustering results given in table I, sec. 2.1. Defect losses during quenching are neglected, and various amounts of clustering which depend upon the quenching temperature, the divacancy binding energy, and the quenching rate are present in the final quenched specimen. Values of the measured total property increment Δp after quenching were calculated under the following two assumptions:

$$\Delta p = p_1 c_1 + 2.0 p_1 c_2 \ , \tag{18}$$

and,

$$\Delta p = p_1 c_1 + 1.8 p_1 c_2 \ . \tag{19}$$

In eq. (19) it is assumed that $p_2 = 1.8p_1$ (i.e., the value of p for an isolated vacant site decreases by 10% when it joins a divacancy). Some results are shown in fig. 12 where the dependency of the Arrhenius plot on the assumptions expressed in eqs. (18) and (19) is shown. The effect of the assumed non-linearity only becomes noticeable at high binding energies where large amounts of clustering are present after quenching. As may be seen maximum differences of about 10% occur in the values of Δp obtained. These results indicate that errors of this magnitude could conceivably be present in the determination of c from Δp data if it is simply assumed that p_n varies linearly with n. Fortunately, the 10% figure calculated above is an extreme value, since it corresponds to both a large amount of clustering and a large assumed non-linearity. The actual importance of this effect in most cases is undoubtedly considerably smaller. For example, in the case of electrical resistivity the resistivity per divacancy is thought to be only ~5% lower than the resistivity due to two well spaced monovacancies [51]. It appears likely, therefore, that eq. (17), with the assumption of constant A, may be used as a reasonably good approximation under most conditions. A possible exception to this is in the measurement of stored energy release in defect systems where large binding energies exist. A major problem in the indirect techniques is the determination of the proportionality factor A in eq. (17). To date, the only direct ways in which this has been accomplished is by comparing quenched-in property changes with either absolute vacancy defect concentrations measured under thermal equilibrium conditions (see, for example, ref. [24]) or total vacancy concentrations measured by transmission electron microscopy (see, for example, ref. [52]). In addition,

approximate values have been obtained from the results of theoretical calculations. We shall not give a detailed discussion of these results here. Instead, we shall focus attention on a number of other complications which exist in the various indirect methods for determining c.

Bulk properties for which such measurements have been made include electrical resistivity, volume or length, and stored energy. A bibliography of much of this work may be found elsewhere [53].

3.3.1. Resistivity measurements

Measurements of electrical resisitivty changes caused by quenching have been used to a great extent since the pioneering experiments of Koehler and coworkers [54]. In terms of measuring quenched-in defect concentrations, measurements of the low temperature electrical resistivity (normally either at 4.2°K or 78°K) are performed on specimens in the well annealed state prior to quenching and then in the as-quenched condition. The difference in these resistivities is then taken to be directly proportional to the total concentration of quenched-in vacant lattice sites. It is normally assumed that Matthiessen's rule, in which the total resistivity can be represented as the sum of a temperature dependent lattice resistivity and a temperature independent point defect contribution [55], is valid: i.e.,

$$\rho = \rho_o(T) + \rho_v \cdot c \quad ,$$

where ρ_v is the resistivity per unit concentration of vacant lattice sites. Although some deviation from Matthiessen's rule may in general be expected, the deviations should be negligible for vacancy defects at 4.2°K. At 78°K,

however, deviations of up to 10% may occur [56,57]. Under most conditions, changes in residual resistivity may therefore be related closely to the total quenched-in vacant site concentrations if the resistivity per unit concentration of vacant sites is known. The advantages of resistivity measurements are the precision with which they can be made, and the fact that the as-quenched state is compared directly with that existing prior to the quench. As such, resistivity measurements provide probably the most accurate method for the comparision of quenched-in total vacancy concentrations from the same quench temperature [50,52].

3.3.2. Volume or length change measurements

Dilatometric measurements have also been used extensively in the study of quenched-in vacant site concentrations in metals (see, for example, refs. [32] and [33]). These investigations, which have been performed on fcc metals, have measured the difference between the specimen length (length changes being related to the isotropic volume changes by $3\frac{\Delta L}{L} = \frac{\Delta V}{V}$) just after quenching to the length after the quenched-in defects have been fully annealed at relatively low temperatures. The observed length change may then, in principle, be related to the quenched-in concentrations if the volume change per vacant site is known. Since in these measurements, in contrast to those utilizing quenched-in resistivity increments, the as-quenched specimen is not related directly to the defect-free specimen prior to quenching, significant additional problems may arise. Here, the quantity measured is $\delta(\Delta\rho)$ which may be written in the form

$$\delta(\Delta\rho) = [\Delta\rho(t = o) - \Delta\rho(t = \infty)],$$

where t is the time of low temperature annealing after quenching. In general, $\Delta p\ (t = \infty) \neq o$ and, therefore, the desired quantity $\Delta p\ (t = o)$ cannot be determined directly. The nature of the vacancy defect annealing e.g., to dislocations or precipitates, can play an important role in determining the value of $\Delta p\ (t = \infty)$. If, as an example of an extreme case, a system of quenched-in vacancy defects having zero lattice relaxation subsequently precipitate in the form of large three-dimensional voids the normal ΔL technique would lead to an apparent conclusion of no quenched-in defects! Another related problem in length change measurements can result from the assumption that an isotropic metal contracts isotropically as the vacancy defects are annihilated at sinks. In the work of Fraikor and Hirth [33] this assumption led to observed apparent vacancy defect concentrations which were considerably smaller than should have been caused by the quenching treatment performed. This anomalous behavior was explained on the basis that their cylindrical single crystal specimens contained a grown-in sub-boundary network consisting primarily of edge dislocations parallel to the axis of the wire. Defect decay to these dislocations then produced an anisotropy in the volume contraction such that very little contraction of the wire length occurred. Clearly, similar effects could also be a problem in the $(\Delta L/L - \Delta a/a)$ technique discussed in sec. 3.2.

3.3.3. Other bulk property measurements

Measurements of changes in properties such as thermoelectric power, and coercive field strength and differential susceptibility in ferromagnetic metals, which are sensitive to the presence of point defects may

also be used in the same sense as electrical resistivity measurements for the measurement of the total quenched-in defect concentration. As they offer no essential departure from the discussion already presented they will not be discussed here further. Calorimetric measurements [58] of the energy stored in specimens quenched from various temperatures, in contrast to other bulk property measurements, enable one to measure the contribution to the property per vacancy, i.e., the formation energy, in the same experiment by determining the stored energy release as a function of quenching temperature. Thus, this technique, in principle, provides a self-contained set of measurements of the total quenched-in vacancy defect concentration if the quenched-in vacancy population consists only of monovacancies. However, it should be emphasized that this measurement is not absolute as are the measurements described in section 3.2. The possibility of significant non-linear p_n behavior (i.e., non-zero cluster binding energies) reduces its value somewhat.

3.4. Measurements sensitive to anisotropic vacancy defect clusters

In addition to the methods discussed above, which are in general applicable to the determination of the concentration of any quenched-in defects, other techniques exist for the measurement of the concentrations of specific defect types which do not have the same symmetry as the lattice in which they exist. These are the measurements of anelastic relaxation and the magnetic after-effect.

3.4.1. Anelastic relaxation measurements

The existence of vacancy clusters in a lattice may give rise to an anelastic relaxation (a reversible time-dependent response in one of the compliance coefficients). This relaxation is due to the repopulation of vacancy clusters among sites which are initially equivalent, but which become nonequivalent under an applied stress. The only defects which give rise to this relaxation are ones which have a group symmetry which is lower than the crystal group symmetry of the host lattice [59]. The strength of the relaxation has been shown by Zener [60] and Nowick and Heller [59] to be proportional to the cluster concentration. Hence, anelastic relaxation measurements are ideally suited for revealing the presence of defects such as divacancies (as originally suggested by R. R. Hasiguti [61]).

The number of reported measurements of this type are surprisingly few, in view of the obvious selectivity of this technique with respect to defect species. The first reported experiments, performed on quenched gold, were by Neuman [62] who failed to find a relaxation which could be clearly attributed to divacancies. Neuman's failure to observe the divacancy peak was largely due to experimental difficulties. He measured a background damping in well annealed gold wire specimens of 6×10^{-4} to 9×10^{-4}, which is quite high when one considers the fact that the strength of the divacancy relaxation was expected to have a value [62] of only $\sim 3c_2$. Okuda and Hasiguti [63] have reported a relaxation in gold at -50°C which was quenched from 1000°C. They attributed this relaxation to the presence of divacancies, but unfortunately they did not measure either the frequency dependence or the concentration dependence of the strength of the relaxation. Hence, the existence of this peak is not firmly established. Very recently

Franklin and Birnbaum [64] have found a relaxation in gold which was quenched, in situ, from 800°C. The strength of the relaxation was found to anneal in the same temperature range as the defect in gold which according to resistivity measurements migrates with an energy of about 0.70eV and which has been tentatively identified as the divacancy [10].

In conclusion, we wish to emphasize the need for carefully planned anelastic relaxation measurements for confirming the presence of higher order vacancy clusters. These measurements must be performed in situ to avoid deforming the specimens, great care should be taken to avoid thermal strains during quenching, and a careful check of the frequency, concentration and orientation dependence of the relaxation must be made to confirm the physical significance of the relaxation.

3.4.2. Magnetic after-effect measurements

Magnetic after-effects, such as the disaccommodation of the initial susceptibility, which are due to the reorientation of defect clusters may also be used to identify different defect species [65]. We note that these measurements are restricted to ferromagnetic metals (e.g., Fe, Ni) and hence represent a rather specialized set of measurements. For a discussion of these experiments the reader is referred to the paper by Kronmüller [66] presented at this conference.

Conclusions:

(1) The only presently available technique for the direct determination of the various c_n is field ion microscopy. This technique has a strong potential for solving a number of outstanding problems concerning vacancy defects. However, several experimental

difficulties must be solved if this potential is to be fully realized.

(2) There is a need for precise direct measurements of the total quenched-in concentration of vacant lattice sites using such techniques as transmission electron microscopy and the simultaneous measurement of length and lattice parameter changes after quenching.

(3) The only data of high accuracy which are available are from measurements of property changes, Δp, due to the quenched-in defects. Of these measurements, those which compare the as-quenched state directly with that existing prior to the quench (e.g., electrical resistivity changes) have the least inherent problems. However, the change in the property per unit concentration of vacant lattice sites, A, must be known, and further careful measurements of these quantities are needed.

(4) Selective indirect measurements which are sensitive to the symmetry difference between a defect cluster and its host lattice (e.g., anelastic relaxation measurements) can provide important information regarding the concentrations, and nature, of the specific quenched-in defects.

4. Determination of formation energies and entropies

In principle, if measurements of the equilibrium concentrations of the c_n are available as a function of T, the $E_n^f(T)$ and $S_n^f(T)$ may be determined in a straightforward manner. Since we have in equilibrium that

$$c_n(T) = \alpha_n \cdot \exp(S_n^f/k) \cdot \exp(-E_n^f/kT), \tag{20}$$

and the basic thermodynamic relationship

$$\frac{\partial E_n^f(T)}{\partial T} = T \frac{\partial S_n^f(T)}{\partial T}, \tag{21}$$

it is readily shown that

$$E_n^f(T) = -k \frac{\partial \ln c_n}{\partial (1/T)}. \tag{22}$$

The usual plot of $\ln c_n$ versus $1/T$ will then display curvature if $E_n^f(T)$ is significantly temperature dependent, but, in any case, $E_n^f(T)$ may be determined from the local slope of this plot using eq. (22). As noted previously, however, there have been no direct measurements of the c_n, and only the field-ion microscope technique seems to offer hope in this direction. If it could be demonstrated using such a technique that clustering after quenching is insignificant, then the monovacancy properties could be readily determined using the above procedure. However, if significant clustering is present the situation becomes ambiguous since, as shown in section 2.1, clustering during the quench makes the determination of the original cluster distributions at T_q impossible by

any direct technique.†

At the present time the only data of any high accuracy which are available are measurements of total property change increments, Δp, as a function of temperature. As discussed in section 3.3, non-linear effects due to clustering should be relatively small under usual conditions, and therefore, c may be taken to be closely proportioned to Δp. The problem is then reduced to obtaining information about the vacancy defects from Δp data where it is assumed that $\Delta p = A \cdot c$ and A is assumed independent of c. If an Arrhenius plot of ln Δp versus 1/T is constructed, it might be hoped that information could be obtained from its shape. Curvature of such a plot could be expected if:

(1) appreciable concentrations of clusters were present in thermal equilibrium at T_q;

(2) only monovacancies were present, but E_1^f (and S_1^f) were appreciably temperature dependent.

These possibilities could lead to confusion in the interpretation of the plot, and it is therefore important to estimate the magnitudes of the curvature which could arise from these effects separately.

---

† We emphasize that we are concerned in this paper with the information which can be obtained from quenching experiments per se. It may, of course, be possible to deduce original cluster distributions using certain models and assumptions regarding the clustering kinetics during the quench. However, a considerable amount of additional information is then required; e.g., the diffusivities of the defects.

4.1. Arrhenius plot curvature due to thermal equilibrium cluster populations

We consider here only the relatively simple case where divacancies constitute the only significant clusters present. Under these conditions

$$c = c_1 + 2c_2 = c_1 + 12c_1^2 \exp(-S_2^b/k)\cdot\exp(E_2^b/kT), \quad (23)$$

or,

$$c = c_1 \{1 + 12 \exp[(S_1^f - S_2^b)/k]\cdot\exp[(E_2^b - E_1^f)/kT]\} . \quad (24)$$

Values of $\Delta p = A\cdot c$ as a function of $1/T$ were calculated for a range of possible parameters, and the results are shown in fig. 13. As expected, the second term in eq. (24), representing the divacancy contribution to the total concentration, makes a contribution at the higher temperatures which increases with an increase in either the quantity $(S_1^f - S_2^b)$ or $(E_2^b - E_1^f)$. The divacancy contributions are appreciable at the higher temperatures for the higher divacancy binding energies and are seen to produce noticeable curvature in these cases. We note that the curves shown in fig. 13 (and in the following fig. 14) are arranged arbitrarily on the vertical scale and are presented mainly to demonstrate how the curves change <u>shape</u> and <u>slope</u> as the assumed defect parameters are varied. (It is instructive in the present context to sight along these curves or to lay a straight edge along them in order to better observe any curvature). We estimate that the curvature in Group 3 ($S_1^f = 0$) would be too small to detect experimentally. In Group 2 ($S_1^f = 1k$) curvature might be

detectable for $E_2^b > 0.3$eV, while for Group 3 ($S_1^f = 2k$) curvature might be detectable for $E_2^b > 0.2$eV. However, extremely high precision data would be required over a wide temperature range. These values are physically possible, and therefore, we may conclude that barely detectable curvatures in the Arrhenius plot could conceivably arise due to the presence of equilibrium divacancies under certain conditions. It is noted that the plot of the experimental data for gold in fig. 7 shows slight positive curvature which may possibly lie outside experimental uncertainty. It is interesting to speculate that this may provide support for the relatively high divacancy binding energy model of Wang, et al. [10] for gold. Similar phenomena might be expected due to the presence of higher order clusters if the binding entropies and energies are of the necessary magnitudes.

4.2. Arrhenius plot curvature due to temperature dependent energies and entropies of formation

We consider the simple case where only monovacancies are present and where S_1^f and E_1^f are temperature dependent. Following the recent treatment by Nowick and Dienes [67] we assume that E_1^f is not strongly dependent upon temperature and use a first order expansion of E_1^f in the form

$$E_1^f(T) = E_1^f(T_o) + B(T - T_o) \quad , \tag{25}$$

where T_o is a reference temperature, and B is a constant. Since it is thermodynamically necessary that $S_1^f = -(\partial G_1^f/\partial T)_p$, it follows that

$$S_1^f(T) = S_1^f(T_o) + B \ln (T/T_o). \tag{26}$$

Using eqs. (25) and (26), we therefore have

$$c_I = \exp\left\{\frac{S_I^f(T_o) + B \ln (T/T_o)}{k}\right\} \cdot \exp\left\{\frac{-[E_I^f(T_o) + B(T - T_o)]}{kT}\right\} . \tag{27}$$

Nowick and Dienes have shown, using quite reasonable thermodynamic estimates, that almost certainly

$$|B| \leq 1.0k \quad . \tag{28}$$

Flynn [68] has given an approximate expression recently for the temperature dependence of the free energy of formation of a vacancy which involves mainly the temperature dependence of the elastic shear modulus. We have used the elastic data of Chang and Himmel [69] for the noble metals to evaluate typical temperature dependences of E_I^f from Flynn's work, and we find temperature dependences which are in the same range as those predicted by Nowick and Dienes [67], i.e., $|B| < k$. Values of $\Delta p = A \cdot c_I$ as a function of $1/T$ were therefore calculated using eq. (27) for different values of B consistent with eq. (28) taking $T_o = 298°K$, $E_I^f(T_o) = 0.94eV$ and $S_I^f(T_o) = 0$. The results are shown in fig. 14. Some positive curvature which increases with B is evident. However, the curvature is relatively small, and is undoubtedly below the level of detection by present methods.

4.3. Discussion

The above results show that there are definite limits to the information which can be obtained from Arrhenius plots of $\ln \Delta p$ versus $1/T$.

If detectable curvature is found, the presence of relatively high concentrations of equilibrium clusters is indicated. On the other hand, if no detectable curvature is observed it can not be concluded that the formation energy is temperature independent or that the effects of clusters are insignificant and that the results should be interpreted solely on the basis of monovacancies. For example, if apparent monovacancy formation energies are derived from the average slopes of the various curves in fig. 13, which do not exhibit detectable curvature, results which differ by as much as 5% are obtained. Similarly, results differing by as much as 7% are obtained from the curves in fig. 14. It may be concluded that errors of this magnitude (or less) could result if the a priori assumption is made that the slope is proportional to a temperature independent monovacancy formation energy.

It need hardly be added that entropies of formation can only be derived when concentration data are available, i.e., the value of A in the relation $\Delta p = A \cdot c$ must be known.

It is clear that detailed and unambiguous information about the vacancy defects present in quenched systems cannot be obtained from quenching experiments which consist of measurements of c only. Measurements of the concentrations, c_n, of the different types of vacancy defect clusters which may be present are urgently required. In certain cases additional information from other types of experiments (e.g., annealing experiments and diffusion experiments) may be used in attempts to interpret quenching experiments. Further discussion of these possibilities is given elsewhere in this conference.

Conclusions:

(1) If the c_n are known as a function of T, $E_n^f(T)$ (and $S_n^f(T)$) may be obtained in a simple manner from the local slope of the Arrhenius plot.

(2) Unfortunately, it has not been possible to obtain appropriate absolute c_n data, and generally the only data of any high accuracy which are available are measurements of total defect property changes, Δp, due to the quenched-in defects. It is usually a good approximation to assume that Δp is proportional to the total concentration of vacant sites, c.

(3) Large defect cluster populations present in equilibrium at high temperatures may cause observable curvature of a ln Δp versus 1/T plot. However, the absence of observable curvature does not necessarily mean that cluster concentrations were negligible, and that the data can be interpreted soley in terms of monovacancies. The determination of an apparent value of E_1^f from the slope of such a curve, differing significantly from the actual value, could result.

(4) It is unlikely that detectable curvature in a plot of ln Δp versus 1/T can result from the temperature dependence of $E_1^f(T)$. However, the average slope of such a curve (and hence the average apparent value of E_1^f) may depend significantly upon the temperature dependence of $E_1^f(T)$.

(5) Entropies of formation can only be derived from concentration data (i.e., the value of A in the relation $\Delta p = A \cdot c$ must be known). There is, in general, an urgent need for absolute measurements of the c_n as a function of temperature.

References

1) M. Doyama, Lattice defects in quenched metals, edited by R. M. J. Cotterill, et al. (Academic Press, New York, 1965) p. 163

2) H. Fujiwara, Technical report, Contract Nonr 1834 (12) 46-22-55-363, Department of Physics, University of Illinois, Urbana, Illinois

3) J. S. Koehler, M. de Jong and F. Seitz, J. Phys. Soc. Japan 18, Supplement III (1963) I

4) R. M. J. Cotterill, Lattice defects in quenched metals, edited by R. M. J. Cotterill, et al. (Academic Press, New York, 1965) p. 97

5) M. Meshii, J. A. McComb, K. Y. Chen, and T. H. Mori, The nature of small defects, edited by M. J. Makin (H. M. Stationery Office, 1966) p. 84

6) F. W. Young, Jr., T. O. Baldwin and F. A. Sherill, Lattice defects and their interactions, edited by R. R. Hasiguti (Gordon and Breach, New York, 1967) p. 543

7) C. P. Flynn, J. Bass and D. Lazarus, Phil. Mag. 11 (1965) 521

8) T. Mori, M. Meshii and J. W. Kauffman, J. Appl. Phys. 33 (1962) 2776

9) T. Kino and J. S. Koehler, Phys. Rev. 162 (1967) 632

10) C. G. Wang, D. N. Seidman and R. W. Balluffi, Phys. Rev. 169 (1968) 553

11) J. J. Jackson, Lattice defects in quenched metals, edited by R. M. J. Cotterill, et al. (Academic Press, New York, 1965) p. 467

12) J. Bass, Phil Mag. 15 (1967) 717

13) R. Gripshover, J. Zetts and J. Bass, this volume

14) K. H. Lie and R. W. Balluffi, to be published

15) D. N. Seidman and R. W. Balluffi, Lattice defects and their interactions, edited by R. R. Hasiguti (Gordon and Breach, New York, 1967) p. 911

16) D. N. Seidman and R. W. Balluffi, Phys. Stat. Sol. 17 (1966) 531

17) D. N. Seidman and R. W. Balluffi, Phys. Rev. 139 (1965) A1824

18) R. W. Balluffi, Interactions between dislocations and point defects, edited by B. L. Eyre (H. M. Stationery Office, to be published)

19) C. P. Flynn, Phys. Rev. 134 (1964) A241

20) F. S. Ham, J. Appl. Phys. 30 (1959) 915

21) K. P. Chik, D. Schumacher and A. Seeger, Phase stability in metals and alloys, edited by P. S. Rudman, et al. (McGraw-Hill, New York, 1967) p. 449

22) A. Seeger and H. Mehrer, Phys. Stat. Sol. 29 (1968) 231

23) J. J. Jackson, Lattice defects in quenched metals, edited by R. M. J. Cotterill, et al. (Academic Press, New York, 1965) p. 479

24) R. O. Simmons and R. W. Balluffi, Phys. Rev. 125 (1962) 862

25) J. Bass, Phys. Rev. 137 (1965) A765

26) C. J. Meechan and R. R. Eggleston, Acta Met. 2 (1954) 680

27) D. N. Seidman and R. W. Balluffi, Phil. Mag. 10 (1964) 1067

28) W. H. Aarts and R. K. Jarvis, Acta Met. 2 (1954) 87

29) Z. S. Basinski, J. S. Dugdale and A. Howie, Phil. Mag. 8 (1963) 1989

30) A. L. Ruoff and R. W. Balluffi, J. Appl. Phys. 34 (1963) 2862

31) A. Ascoli, M. Asdente, E. Germagnoli, and A. Manara, J. Phys. Chem. Solids 6 (1958) 59

32) J. Takamura, Lattice defects in quenched metals, edited by R. M. J. Cotterill, et al. (Academic Press, New York, 1965) p. 521

33) F. J. Fraikor and J. P. Hirth, J. Appl. Phys. 38 (1967) 2312

34) E. W. Müller, University of Florida short course on field ion microscopy (Metallurgical Engineering Department, Gainsville, Florida, 1966)

35) O. Nishikawa and E. W. Müller, J. Appl. Phys. 35 (1964) 2806

36) J. F. Mulson and E. W. Müller, J. Chem. Phys. 38 (1963) 2615

37) E. W. Müller, Advances in electronics and electron physics, edited by L. Marton (Academic Press, New York, 1960) Vol. 13, p. 83

38) B. I. Bleany and B. Bleany, Electricity and magnetism (Oxford University Press, London, 1957) p. 28

39) A. I. Lur'e, Three dimensional problems of the theory of elasticity (Interscience, New York, 1964)

40) R. L. Schwoebel, J. Appl. Phys. 38 (1967) 3154

41) R. M. Emrick, Phys. Rev. 122 (1961) 1720

42) S. S. Brenner, United States Steel Corporation Report PR300 (1965); S. S. Brenner, High temperature, high resolution microscopy (Gordon and Breach, New York, 1968)

43) R. M. Scanlan, D. N. Seidman, D. L. Styris and D. G. Ast, Cornell University Materials Science Center Report (1968)

44) Bubble and spark chambers, edited by R. P. Shutt (Academic Press, New York, 1967) Vol. 2

45) E. W. Müller, Z. Physik 156 (1959) 399

46) C. A. Speicher, W. T. Pimbley, M. J. Attardo, J. M. Galligan and S. S. Brenner, Phys. Lett. 23 (1966) 194

47) D. G. Ast and D. N. Seidman, Cornell University Materials Science Center Report #1025, to appear Appl. Phys. Letters, 15 Nov. (1968)

48) R. M. J. Cotterill, Phil. Mag. 6 (1961) 1351

49) M. Meshii, Lattice defects in quenched metals, edited by R. M. J. Cotterill, et al. (Academic Press, New York, 1965) p. 387

50) R. W. Siegel, Phil. Mag. 13 (1966) 337

51) C. P. Flynn, J. Phys. Radium 23 (1962) 654

52) R. W. Siegel, Phil. Mag. 13 (1966) 359

53) Lattice defects in quenched metals, edited by R. M. J. Cotterill, et al. (Academic Press, New York, 1965)

54) J. E. Bauerle and J. S. Koehler, Phys. Rev. 107 (1957) 1493; J. W. Kauffman and J. S. Koehler, Phys. Rev. 88 (1952) 149

55) J. M. Ziman, Electrons and phonons (Oxford University Press, London, 1960) p. 337

56) H. Bross, Z. Naturforsch. 14a (1959) 560

57) R. R. Conte, J. Dural and Y. Quéré, this volume

58) W. DeSorbo, Phys. Rev. 117 (1960) 444

59) A. S. Nowick and W. R. Heller, Advanc. Phys. 12 (1963) 251

60) C. A. Zener, Elasticity and anelasticity of metals (University of Chicago Press, Chicago, 1948) p. 137

61) R. R. Hasiguti, J. Phys. Soc. Japan 8 (1953) 798

62) C. H. Neuman, Ph.D. Thesis (Physics), University of Illinois (1963); C. H. Neuman, J. Phys. Chem. Solids 27 (1966) 427

63) S. Okuda and R. R. Hasiguti, J. Phys. Soc. Japan 19 (1964) 242

64) D. Franklin and H. K. Birnbaum, University of Illinois, private communication (1968)

65) H. Rieger, Z. Metallk. 54 (1963) 229; H. Rieger, H. Kronmüller, and A. Seeger, ibid. 54 (1963) 553; H. Jäger, ibid. 55 (1964) 17

66) H. Kronmüller, this volume

67) A. S. Nowick and G. J. Dienes, Phys. Stat. Sol. 24 (1967) 461

68) C. P. Flynn, Phys. Rev. 171 (1968) 682

69) Y. A. Chang and L. Himmel, J. Appl. Phys. 37 (1966) 3567

Table I. The ratio of divacancies to monovacancies (c_2/c_1) frozen-in at low temperatures after linear quenches from T_q for a closed monovacancy-divacancy system with $E_1^f = 0.94eV$, $E_1^m = 0.90eV$, $S_1^f = 0$, $S_2^b = 0$ (i.e., the divacancy binding entropy) and $\nu = 10^{13}\ sec^{-1}$.

$T_q = 500^oC$; $c = 0.075 \times 10^{-5}$

E_2^b(eV)	c_2/c_1		
	quenching rate ($^oC \cdot sec^{-1}$)		
	10^3	10^4	10^5
0.10	0.807×10^{-4}	0.658×10^{-4}	0.537×10^{-4}
0.20	0.879×10^{-3}	0.595×10^{-3}	0.400×10^{-3}
0.30	0.656×10^{-2}	0.388×10^{-2}	0.227×10^{-2}
0.40	0.359×10^{-1}	0.188×10^{-1}	0.098×10^{-1}

$T_q = 700^oC$; $c = 1.35 \times 10^{-5}$

E_2^b(eV)	c_2/c_1		
	quenching rate ($^oC \cdot sec^{-1}$)		
	10^3	10^4	10^5
0.10	0.146×10^{-2}	0.118×10^{-2}	0.950×10^{-3}
0.20	0.157×10^{-1}	0.107×10^{-1}	0.726×10^{-2}
0.30	0.107	0.654×10^{-1}	0.394×10^{-1}
0.40	0.469	0.276	0.157

Table I (continued)

$T_q = 900^{\circ}C$; $c = 9.18 \times 10^{-5}$

E_2^b (eV)	c_2/c_1		
	quenching rate ($^{\circ}C \cdot sec^{-1}$)		
	10^3	10^4	10^5
0.10	0.974×10^{-2}	0.788×10^{-2}	0.638×10^{-2}
0.20	0.961×10^{-1}	0.673×10^{-1}	0.468×10^{-1}
0.30	0.520	0.345	0.224
0.40	0.844	1.184	0.744

Table 2. Calculated [a] maximum plastic shear strain in gold wires due to internal thermal stresses after linear quenching into water.

Wire dia. (cm)	Max. heat flux removed in quench ($cal \cdot cm^{-2} \cdot sec^{-1}$)	Max. cooling rate ($°C \cdot sec^{-1}$)	Shear strain ($X10^5$)
0.041	240	40×10^3	1.5
0.152	225	10×10^3	8.5
0.317	210	4.6×10^3	25.

[a] all data from reference [23]

Table 3. Calculated [a] hydrodynamic stretching strain in initially straight 10.2 cm long gold wire after fast quenching [b] in water.

Wire dia (cm)	Stretching Strain ($X10^4$)
0.0051	33.5
0.0102	21.1
0.0203	13.2
0.0406	8.3
0.0813	5.5
0.163	3.3
0.325	1.4

a) All data from reference [23]

b Fast quenching refers to the use of a characteristic optium velocity of the specimen to the water (see reference [23] for complete discussion).

Table 4. The quantity $\Delta R(\varepsilon)/\Delta R(0)$ determined experimentally after quenching strained and unstrained 0.041 cm dia platinum wires from various temperatures.[a)]

Plastic shear strain ($X10^4$)	$\Delta R(\varepsilon)/\Delta R(0)$		
	T_q = 1500°C	T_q = 1200°C	T_q = 900°C
1	0.995	1.00	1.00
3	0.99	1.00	1.00
10	0.96	1.00	1.00
30	0.85	0.98	0.995
70	0.73	0.85	0.96
150	0.68	0.74	0.93
250	0.60	0.69	0.94

a) All data from reference [23)]

Table 5. Effect of the evaporation field on the monovacancy diffusivity [a] in a platinum field ion microscope specimen.

T(°K)	$D_1(p_o,T)$ $(cm^2 \cdot sec^{-1})$	$\exp[\Delta V_1^m \lvert (p - p_o) \rvert / kT]$	$D_1(p,T)$ $(cm^2 \cdot sec^{-1})$
4	2.03×10^{-1766}	1.33×10^{237}	2.71×10^{-1529}
78	1.08×10^{-92}	1.45×10^{12}	1.57×10^{-80}
273	4.46×10^{-28}	2.98×10^{3}	1.33×10^{-24}

a) The monovacancy diffusivity was calculated from eq. (12) taking $\nu = 2 \times 10^{13}$ sec^{-1} and $\Delta G_1^m = 1.40$ eV (ref. [41]). The evaporation field was taken to be 500×10^8 $volts \cdot m^{-1}$. We neglected the $[(\frac{2}{3} - \gamma) \cdot \chi \lvert (p - p_o) \rvert]$ term since it is negligible with respect to $[\frac{\Delta V_1^m}{kT} \lvert (p - p_o) \rvert]$. To evaluate the former term we took $\gamma = 3.3$ and $\chi = 3.6 \times 10^{-13}$ $cm^2 \cdot dyne^{-1}$.

Figure captions

fig. 1. The ratio of divacancies to monovacancies, c_2/c_1, versus temperature during a quench from 700°C for various values of E_2^b and linear quench rate. The curves were calculated using eqs. (2) through (4) for a closed monovacancy-divacancy system with $E_1^f = 0.94$ eV, $E_1^m = 0.90$ eV, $S_1^f = 0$, $S_2^b = 0$ and $\nu = 10^{13}$ sec^{-1}. The arrows indicate values of T^* calculated using eq. (7).

fig. 2. The calculated ratio of divacancies to monovacancies, c_2/c_1, frozen-in after a quench from 700°C as a function of the linear quenching rate for the specific vacancy parameters given. This example shows the large uncertainty in attempting to extrapolate measured c_n data after quenching to obtain the equilibrium c_n values at the quench temperature, T_q (i.e., at infinite quenching rate).

fig. 3. The fractional resistivity quenched into 0.041 cm dia gold wires as a function of quench temperature for various quenching media and, therefore, quenching rates from the work of Flynn, et al. [7]. Quenching times for the various media were in the range 0.025 sec (water) $\leq \tau_q \leq$ 4.3 sec (air).

fig. 4. The quenched-in resistivity increment in gold from two different quench temperatures, T_q = 700°C and 850°C, as a function of quenching rate from the work of Flynn, et al.[7]. This example shows the reliability of the technique of

extrapolating to infinite quenching rate to correct for vacancy losses during quenching.

fig. 5. The quenched-in monovacancy concentration, c_1, as a function of quench temperature for various linear quenching rates. The curves were calculated for a simple monovacancy system with the vacancy parameters shown and with a dislocation sink density of 5×10^7 cm^{-2}.

fig. 6. The quenched-in monovacancy concentration, c_1, as a function of quenching rate for various quench temperatures, T_q. The curves were calculated for a simple monovacancy system with the vacancy parameters shown. Separate curves are shown for losses to subgrain boundaries and dislocations.

fig. 7. The total concentration of vacant lattice sites in gold as a function of temperature as determined by equilibrium measurements [24] and quenched-in electrical resistivity [7-10,12], where the quenched-in increments were obtained by extrapolations to infinite quenching rate. The resistivity data were fitted together using a common temperature scale [26] and the value of $\rho_o(25°C) = 2.25 \times 10^{-6}$ Ω cm (ref. [25]), and were converted to concentrations using 1.5×10^{-6} Ω cm as the resistivity of 1 at.% of vacant sites.

fig. 8. A schematic representation of the stress distribution on a typical field ion microscope specimen tip end form

caused by the imaging field, E. The end form is described by two radii of curvature R and R/2.

fig. 9. The atom by atom dissection of a (334) plane of tungsten initially containing 10 atoms. The configuration and number of atoms remaining are presented schematically below each frame for clarification. The arrows indicate the sites from which the atoms were removed between successive frames. Field micrographs are from unpublished work by R. M. Scanlan, D. L. Styris and D. N. Seidman.

fig. 10. A field ion micrograph of a well developed, stable end form of gold, imaged with a 25% Ne-He gas mixture at ~ 16°K. Micrograph from research of D. G. Ast and D. N. Seidman [47].

fig. 11. A graphic representation of the measurement of the total vacant site concentration, c, by the simultaneous measurement of length and lattice parameter changes after quenching. The curves for $(3\Delta L/L)$ and $(3\Delta a/a)$ have been plotted together so that their asymptotes in the fully annealed state superimpose. The difference between these curves is then equal to c.

fig. 12. The effect of non-linearity of the p_n on the observed ln Δp versus 1/T plot. The curves were calculated for a closed monovacancy-divacancy system using the parameters given. Two cases were considered: (a) the linear case, where $p_2 = 2p_1$, and (b) a non-linear case, where $p_2 = 1.8\ p_1$.

The curves are presented using an arbitrary vertical scale for clarity.

fig. 13. Arrhenius plots of ln ($A \cdot c$) versus 1/T calculated for a monovacancy-divacancy system in thermal equilibrium using eq. (24) with the various vacancy parameters given, showing the variation of curvature and slope as the defect parameters are changed. The curves are presented using an arbitrary vertical scale for clarity.

fig. 14. Arrhenius plots of ln ($A \cdot c_1$) versus 1/T calculated for a monovacancy system with a temperature dependent energy and entropy of formation using eq. (27) with various values of the parameter B consistent with eq. (28). The curves are presented using an arbitrary vertical scale for clarity.

fig. 1

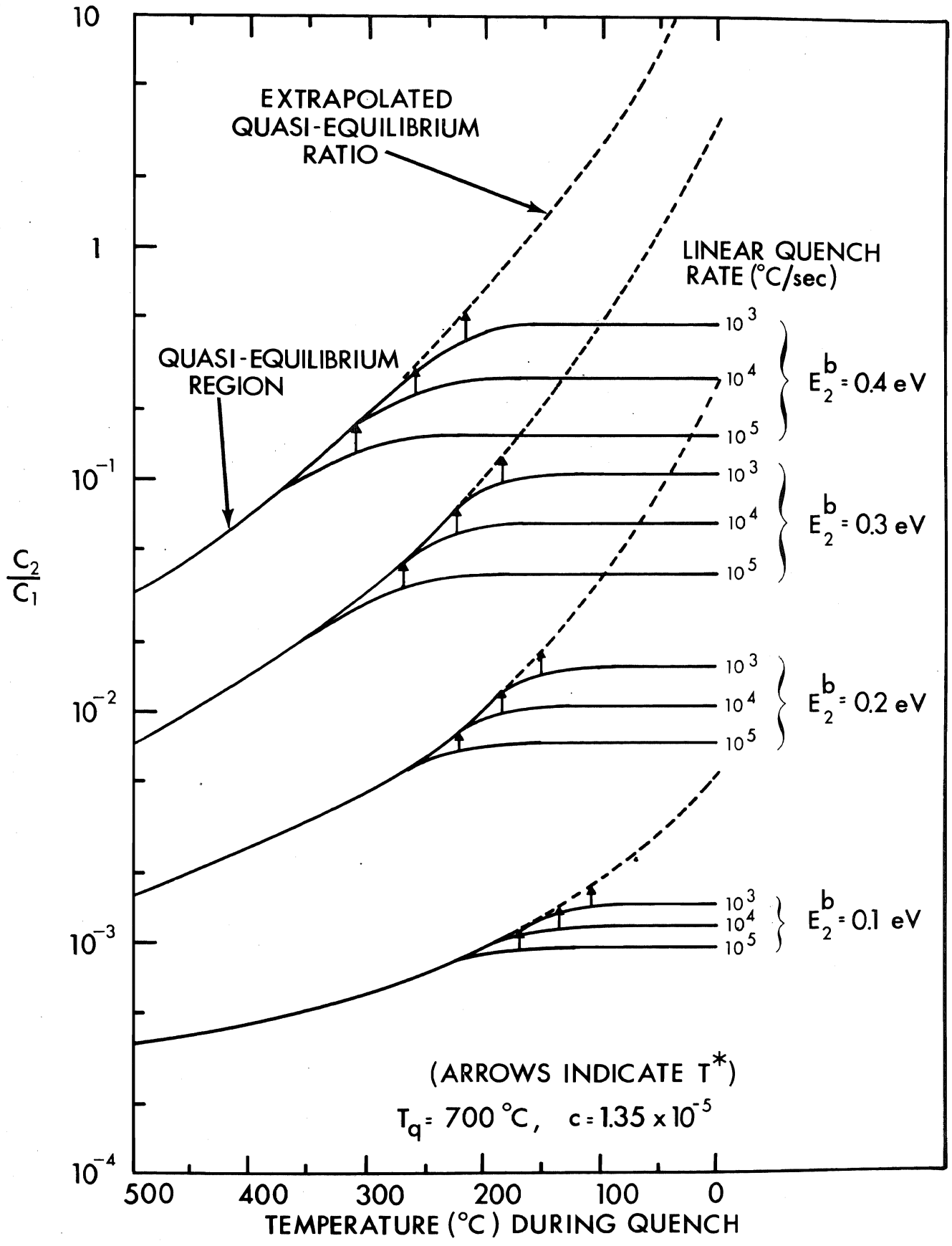
10
1
10^{-1}
10^{-2}
10^{-3}
10^{-4}
$\frac{C_2}{C_1}$
EXTRAPOLATED QUASI-EQUILIBRIUM RATIO
QUASI-EQUILIBRIUM REGION
LINEAR QUENCH RATE (°C/sec)
10^3
10^4
10^5
E_2^b = 0.4 eV
E_2^b = 0.3 eV
E_2^b = 0.2 eV
E_2^b = 0.1 eV
(ARROWS INDICATE T^*)
T_q = 700 °C, $c = 1.35 \times 10^{-5}$
500
400
300
200
100
0
TEMPERATURE (°C) DURING QUENCH

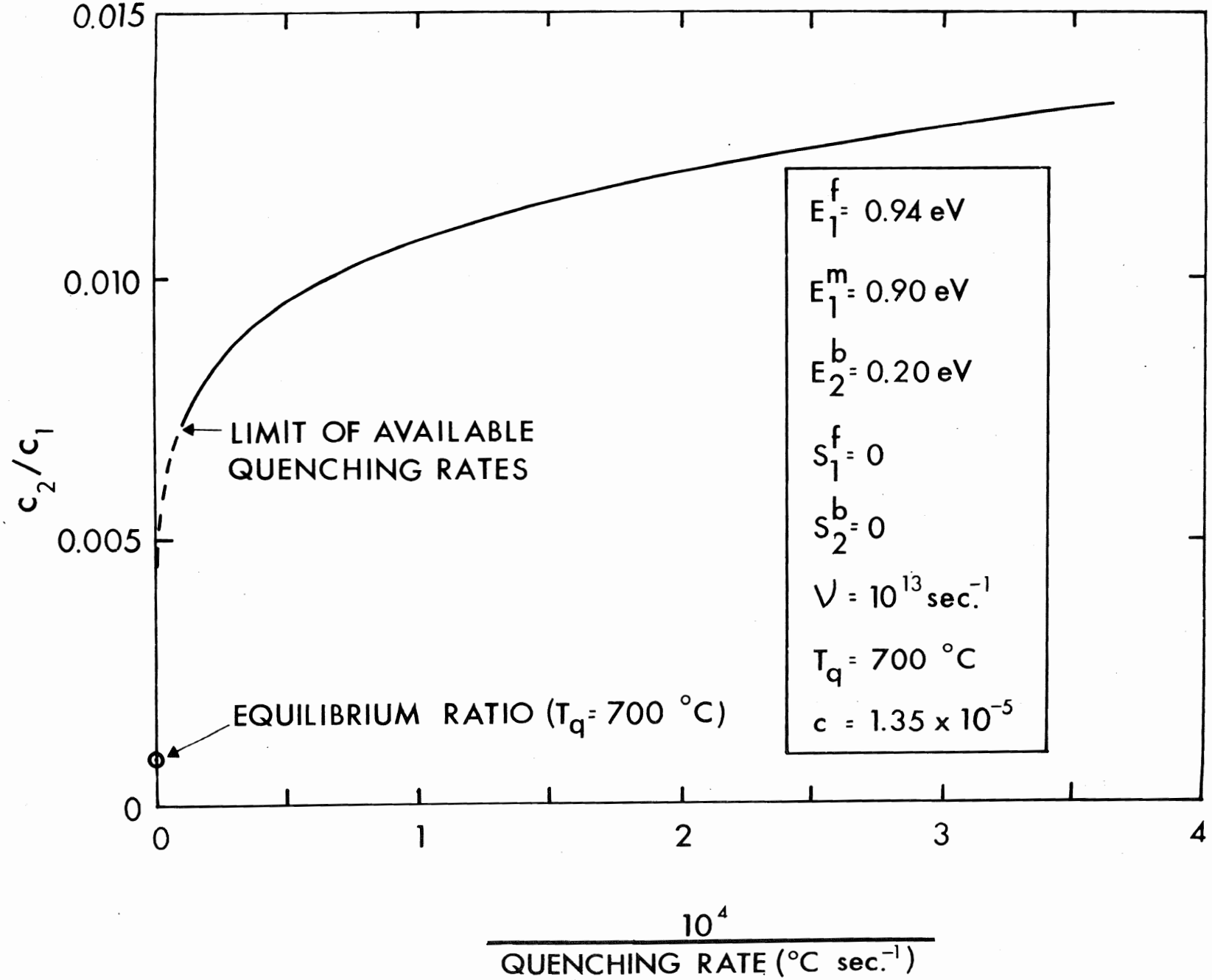
0.015
0.010
0.005
0
c_2/c_1
LIMIT OF AVAILABLE QUENCHING RATES
EQUILIBRIUM RATIO (T_q = 700 °C)
E_1^f = 0.94 eV
E_1^m = 0.90 eV
E_2^b = 0.20 eV
S_1^f = 0
S_2^b = 0
$\nu = 10^{13}$ sec.$^{-1}$
T_q = 700 °C
$c = 1.35 \times 10^{-5}$
0
1
2
3
4
$\frac{10^4}{\text{QUENCHING RATE (°C sec.}^{-1})}$

fig. 2

fig. 3

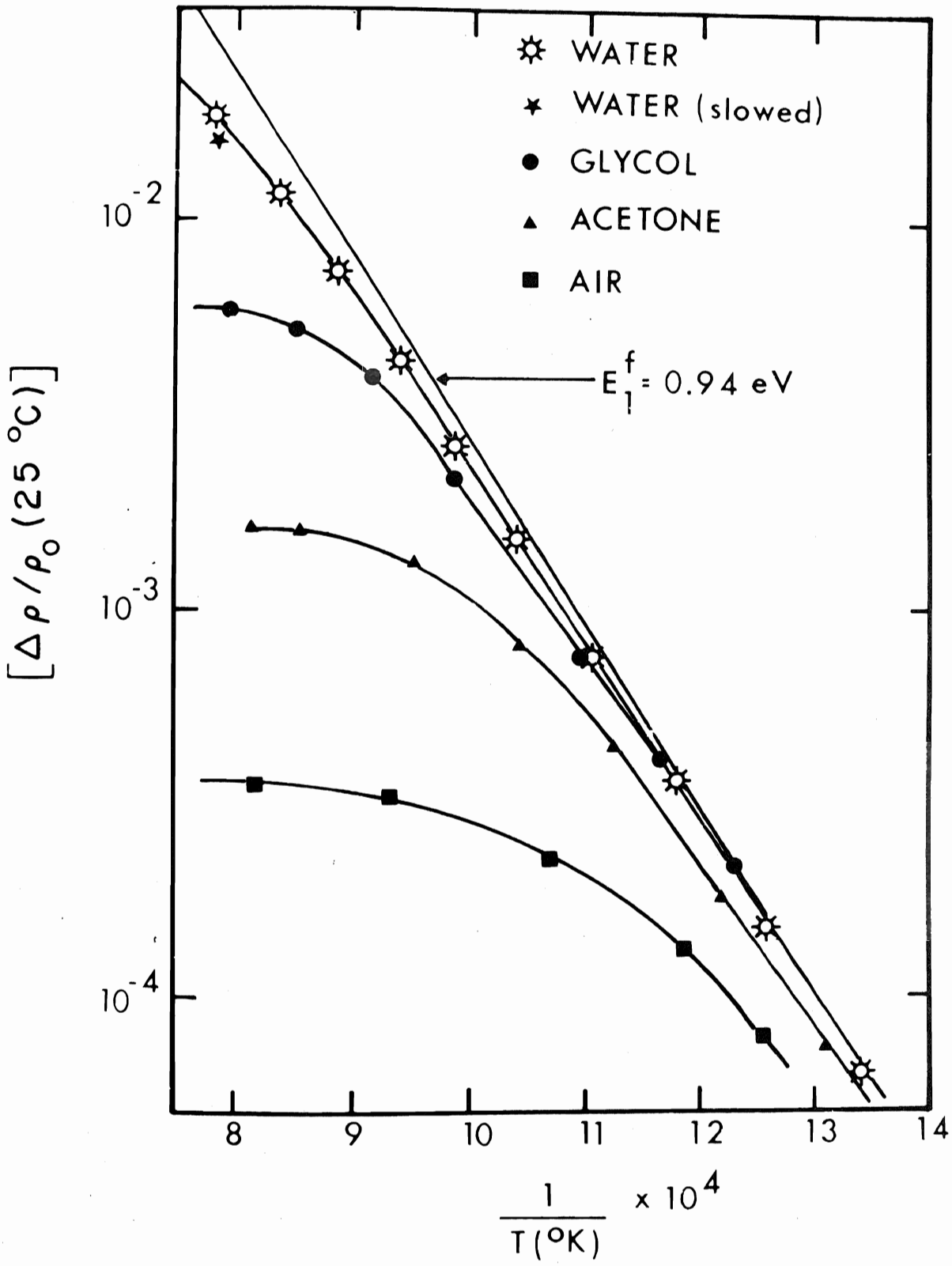
WATER
WATER (slowed)
GLYCOL
ACETONE
AIR
E_1^f = 0.94 eV
$[\Delta\rho/\rho_o(25\ ^oC)]$
10^{-2}
10^{-3}
10^{-4}
8
9
10
11
12
13
14
$\frac{1}{T(^oK)} \times 10^4$

fig. 4

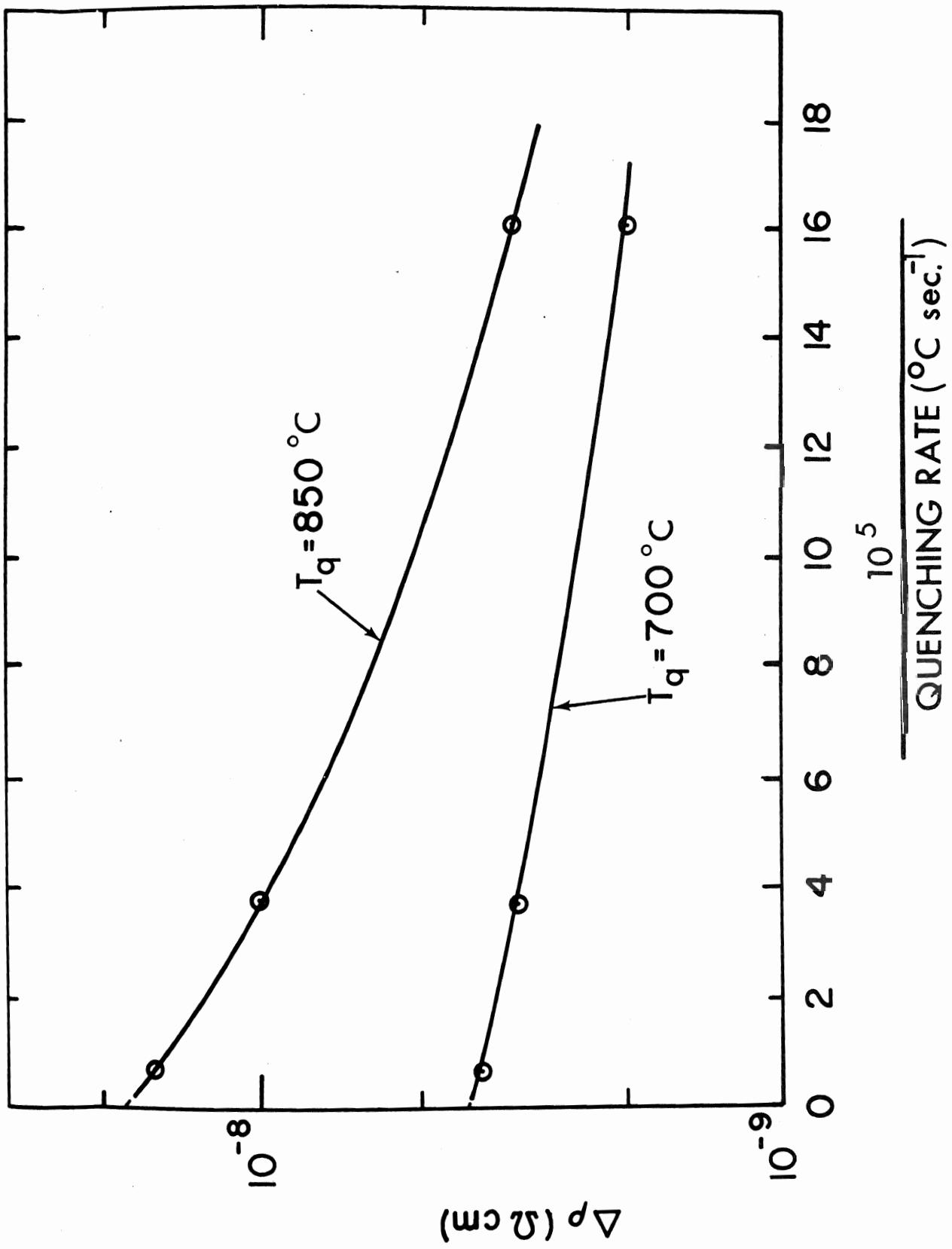
$\Delta\rho$ (Ω cm)
10^{-8}
10^{-9}
T_q=850 °C
T_q=700 °C
0
2
4
6
8
10
12
14
16
18
10^5
QUENCHING RATE (°C sec.$^{-1}$)

fig. 5

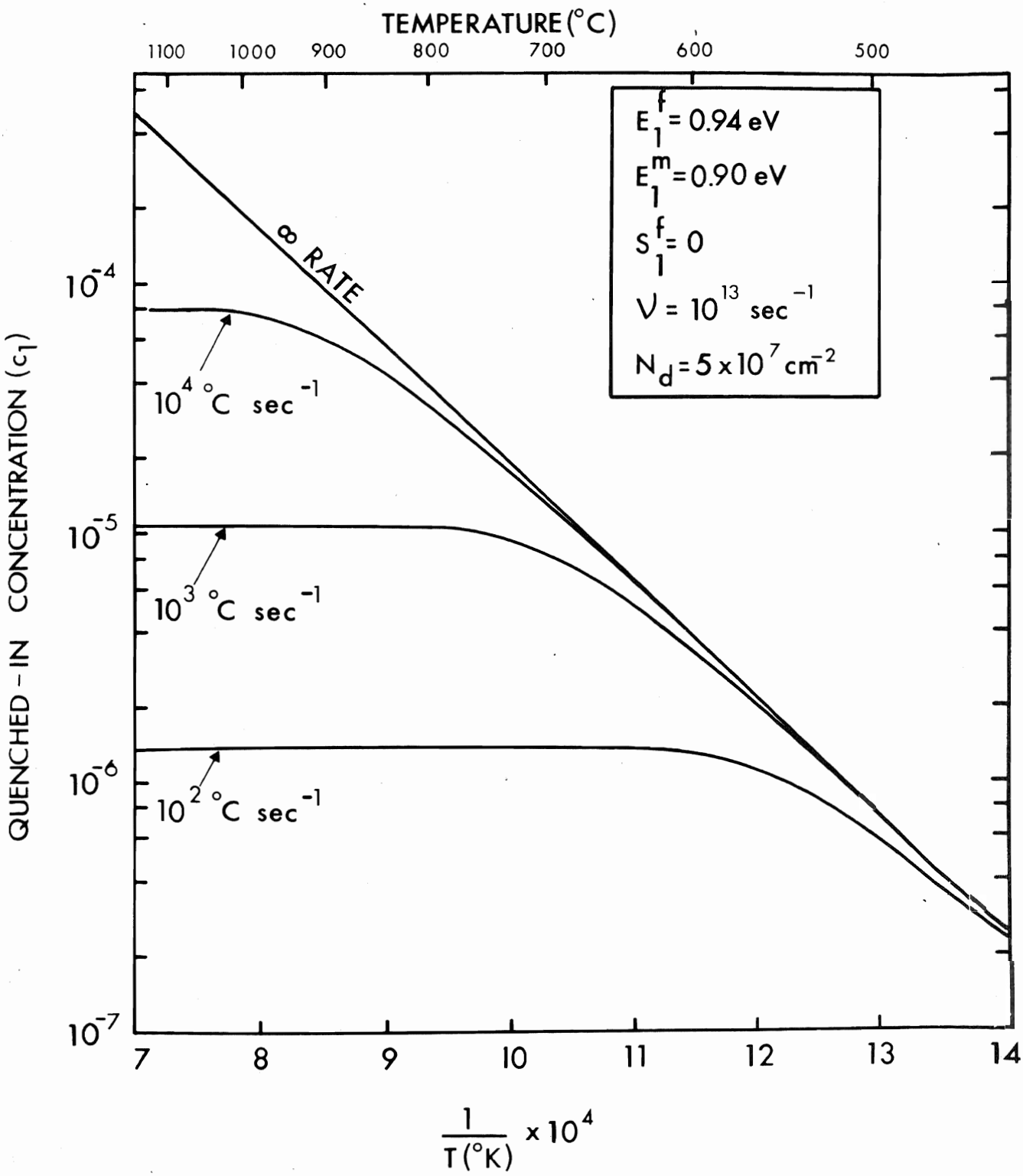
TEMPERATURE (°C)
1100
1000
900
800
700
600
500
$E_1^f = 0.94$ eV
$E_1^m = 0.90$ eV
$S_1^f = 0$
$\nu = 10^{13}$ sec^{-1}
$N_d = 5 \times 10^7$ cm^{-2}
∞ RATE
10^4 °C sec^{-1}
10^3 °C sec^{-1}
10^2 °C sec^{-1}
QUENCHED - IN CONCENTRATION (c_1)
10^{-4}
10^{-5}
10^{-6}
10^{-7}
7
8
9
10
11
12
13
14
$\frac{1}{T(°K)} \times 10^4$

fig. 6

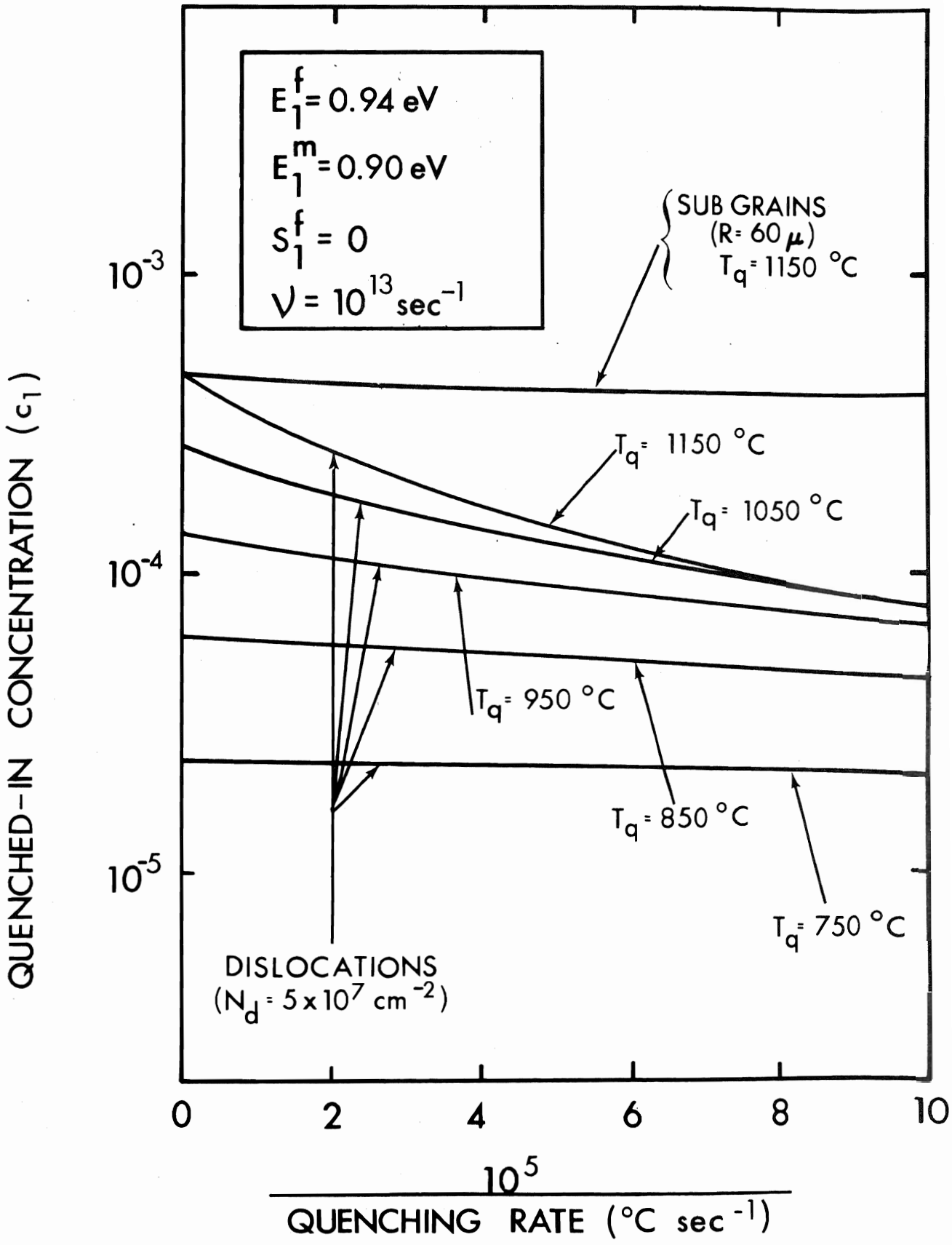
$E_1^f = 0.94$ eV
$E_1^m = 0.90$ eV
$S_1^f = 0$
$\nu = 10^{13}$ sec^{-1}
SUB GRAINS
(R = 60 μ)
T_q = 1150 °C
T_q = 1150 °C
T_q = 1050 °C
T_q = 950 °C
T_q = 850 °C
T_q = 750 °C
DISLOCATIONS
($N_d = 5 \times 10^7$ cm^{-2})
QUENCHED-IN CONCENTRATION (c_1)
10^{-3}
10^{-4}
10^{-5}
0
2
4
6
8
10
10^5
QUENCHING RATE (°C sec^{-1})

fig. 7

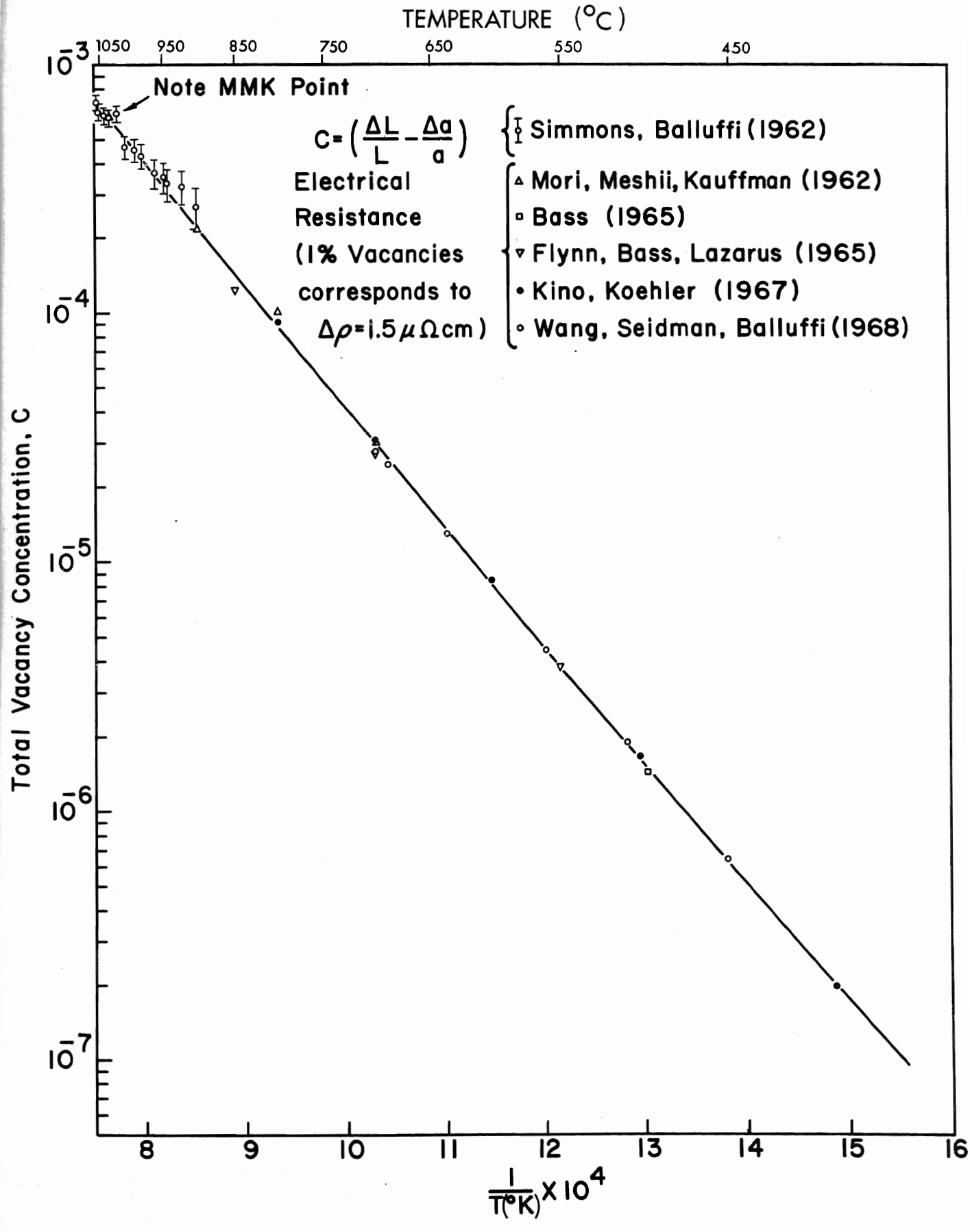
TEMPERATURE (°C)
1050
950
850
750
650
550
450
Note MMK Point
$C=\left(\frac{\Delta L}{L}-\frac{\Delta a}{a}\right)$
Simmons, Balluffi (1962)
Electrical Resistance (1% Vacancies corresponds to $\Delta\rho$=1.5 $\mu\Omega$cm)
Mori, Meshii, Kauffman (1962)
Bass (1965)
Flynn, Bass, Lazarus (1965)
Kino, Koehler (1967)
Wang, Seidman, Balluffi (1968)
Total Vacancy Concentration, C
10^{-3}
10^{-4}
10^{-5}
10^{-6}
10^{-7}
8
9
10
11
12
13
14
15
16
$\frac{1}{T(°K)} \times 10^4$

fig. 8

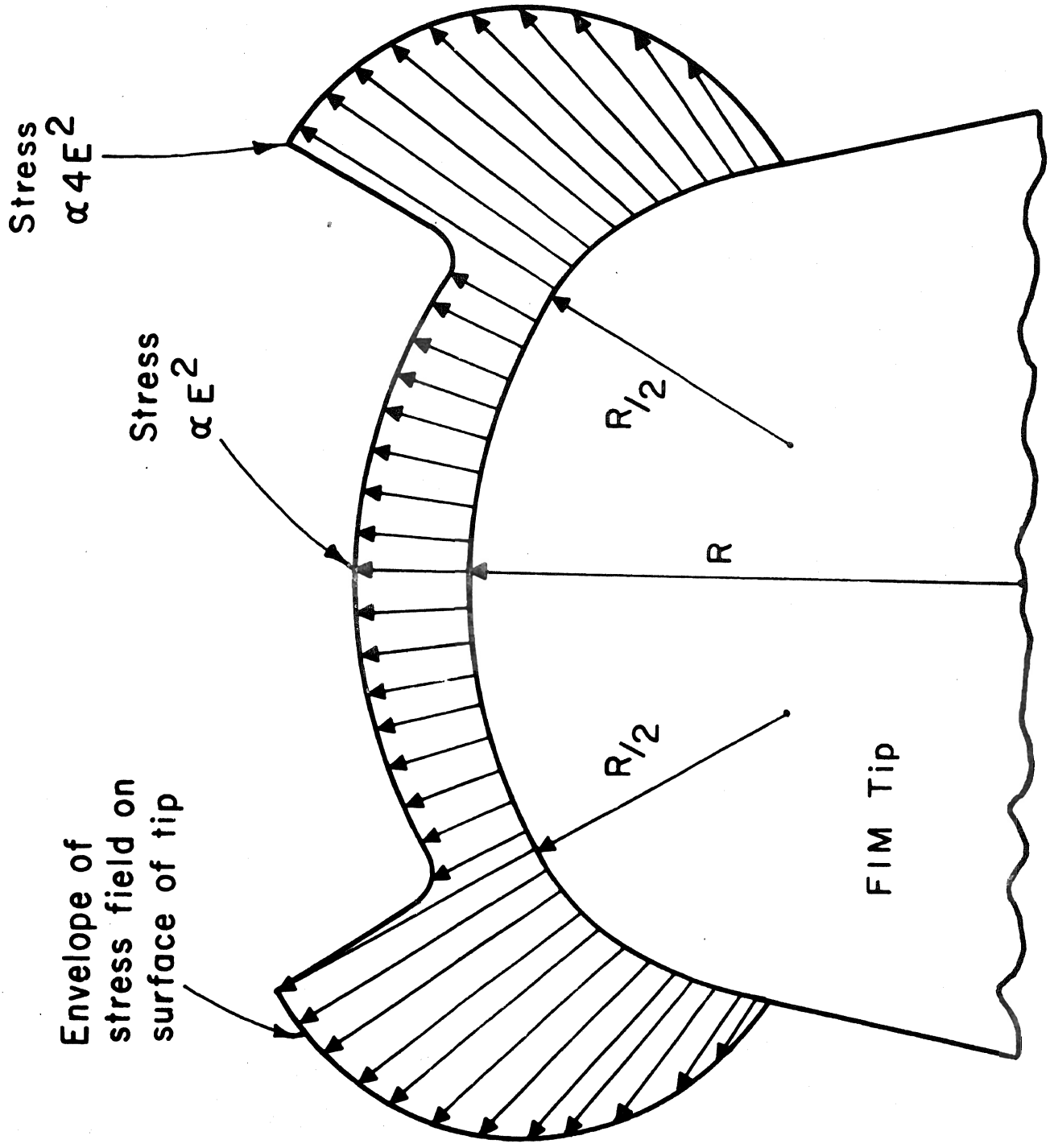
Stress
$\alpha 4E^2$
Stress
αE^2
$R_{1/2}$
R
$R_{1/2}$
Envelope of
stress field on
surface of tip
FIM Tip

1
2
3
4
5
6
8
9
10

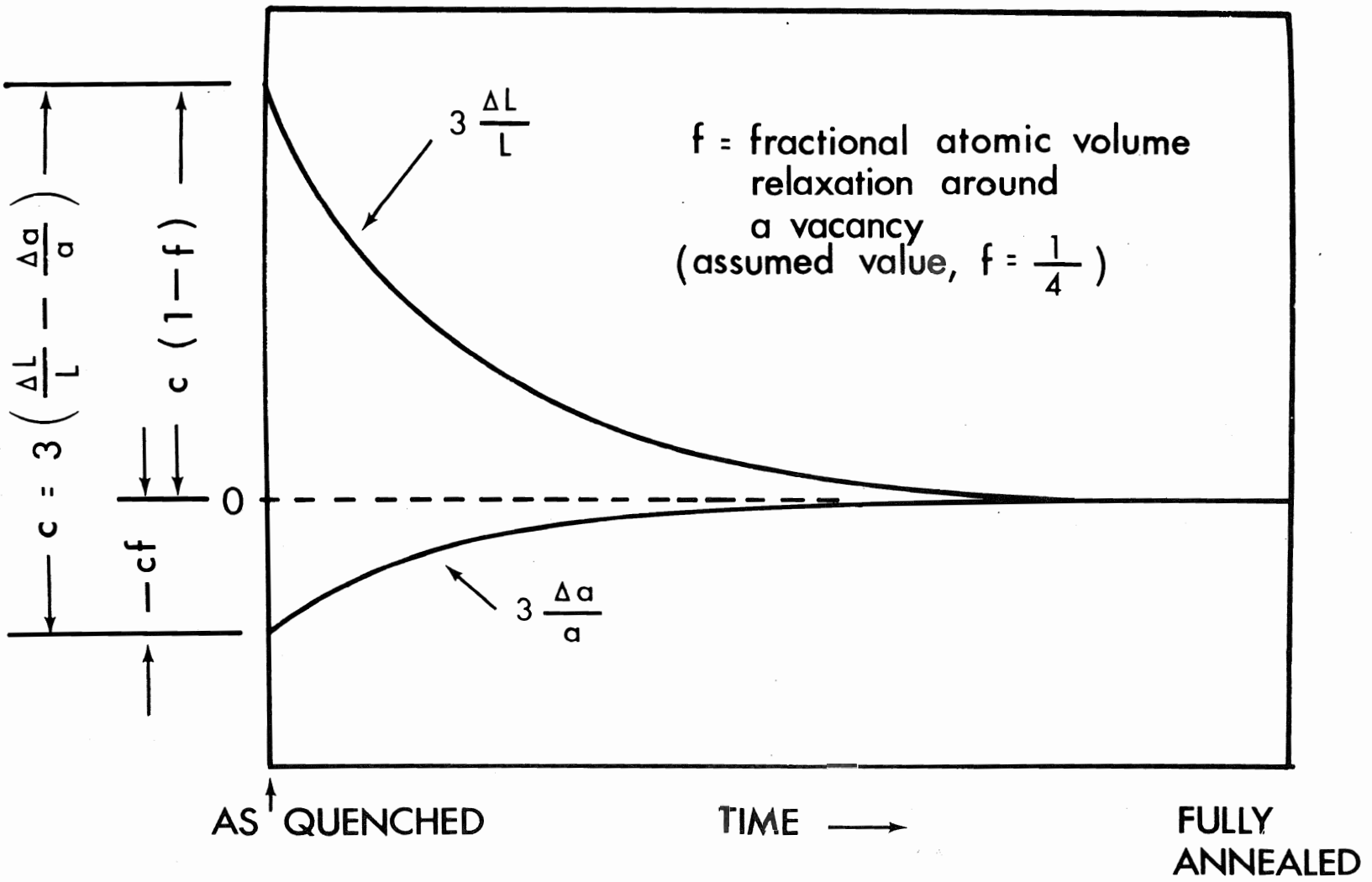
$3\frac{\Delta L}{L}$
f = fractional atomic volume relaxation around a vacancy (assumed value, $f = \frac{1}{4}$)
$c = 3\left(\frac{\Delta L}{L} - \frac{\Delta a}{a}\right)$
$c\,(1-f)$
0
$-cf$
$3\frac{\Delta a}{a}$
AS QUENCHED
TIME
FULLY ANNEALED

fig. 11

fig. 12

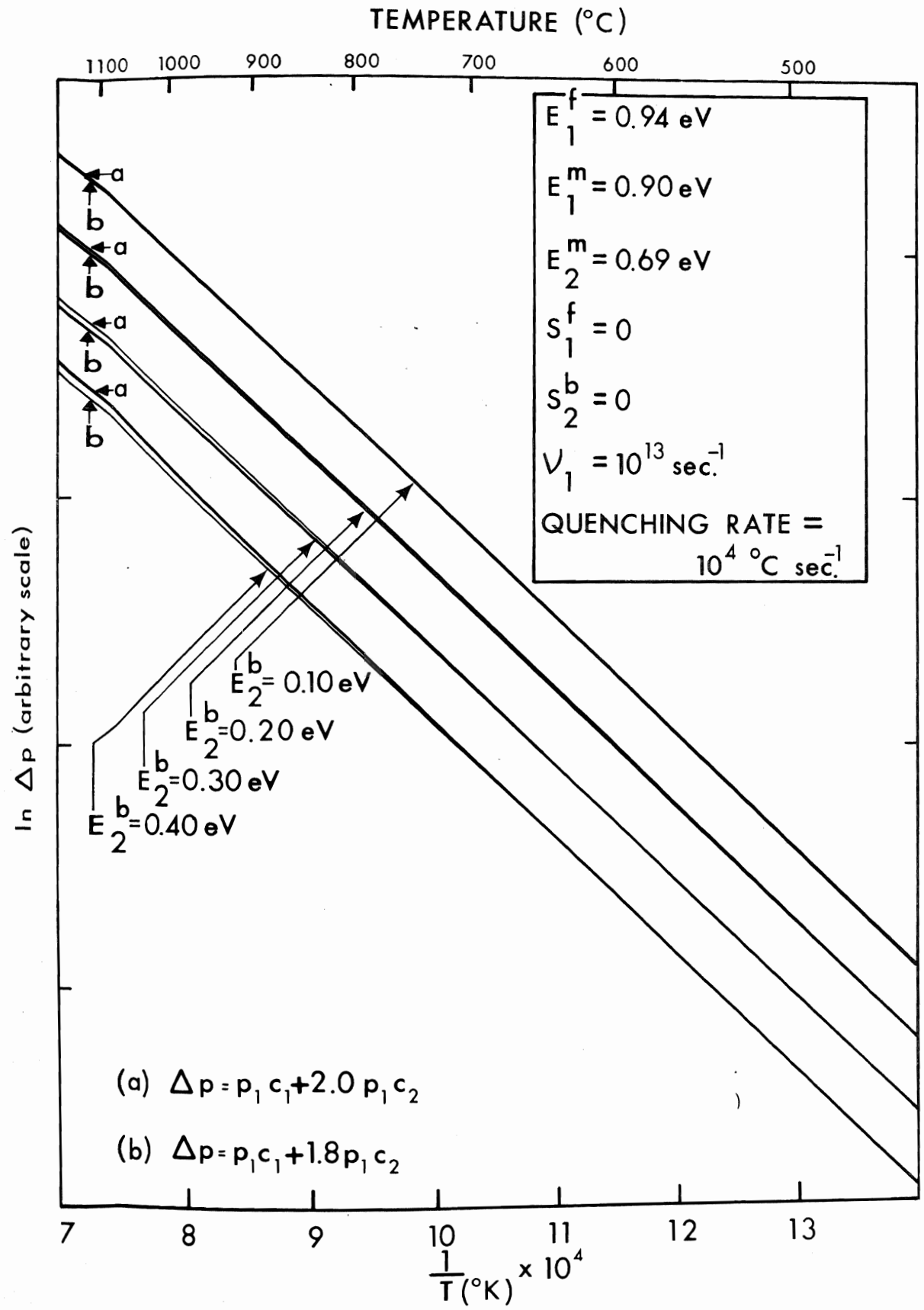
TEMPERATURE (°C)
1100
1000
900
800
700
600
500
E_1^f = 0.94 eV
E_1^m = 0.90 eV
E_2^m = 0.69 eV
S_1^f = 0
S_2^b = 0
ν_1 = 10^{13} sec.$^{-1}$
QUENCHING RATE = 10^4 °C sec.$^{-1}$
a
b
E_2^b= 0.10 eV
E_2^b=0.20 eV
E_2^b=0.30 eV
E_2^b=0.40 eV
ln Δp (arbitrary scale)
(a) $\Delta p = p_1 c_1 + 2.0\, p_1 c_2$
(b) $\Delta p = p_1 c_1 + 1.8\, p_1 c_2$
7
8
9
10
11
12
13
$\frac{1}{T(°K)} \times 10^4$

fig. 13

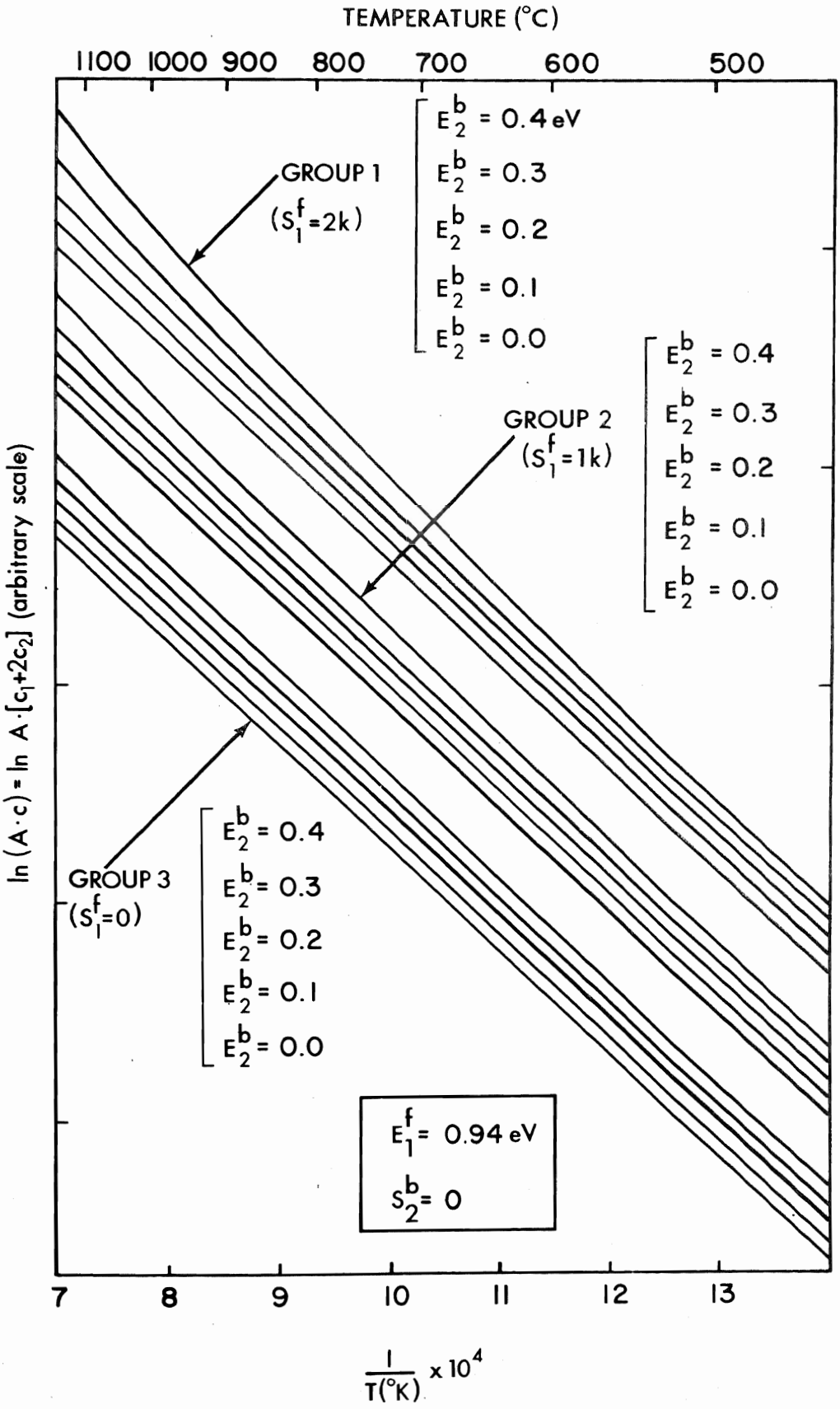
TEMPERATURE (°C)
1100 1000 900 800 700 600 500
GROUP 1
(S_1^f=2k)
E_2^b = 0.4 eV
E_2^b = 0.3
E_2^b = 0.2
E_2^b = 0.1
E_2^b = 0.0
GROUP 2
(S_1^f=1k)
E_2^b = 0.4
E_2^b = 0.3
E_2^b = 0.2
E_2^b = 0.1
E_2^b = 0.0
GROUP 3
(S_1^f=0)
E_2^b = 0.4
E_2^b = 0.3
E_2^b = 0.2
E_2^b = 0.1
E_2^b = 0.0
E_1^f = 0.94 eV
S_2^b = 0
ln (A·c) = ln A·[c_1+2c_2] (arbitrary scale)
7 8 9 10 11 12 13
$\frac{1}{T(°K)} \times 10^4$

fig. 14

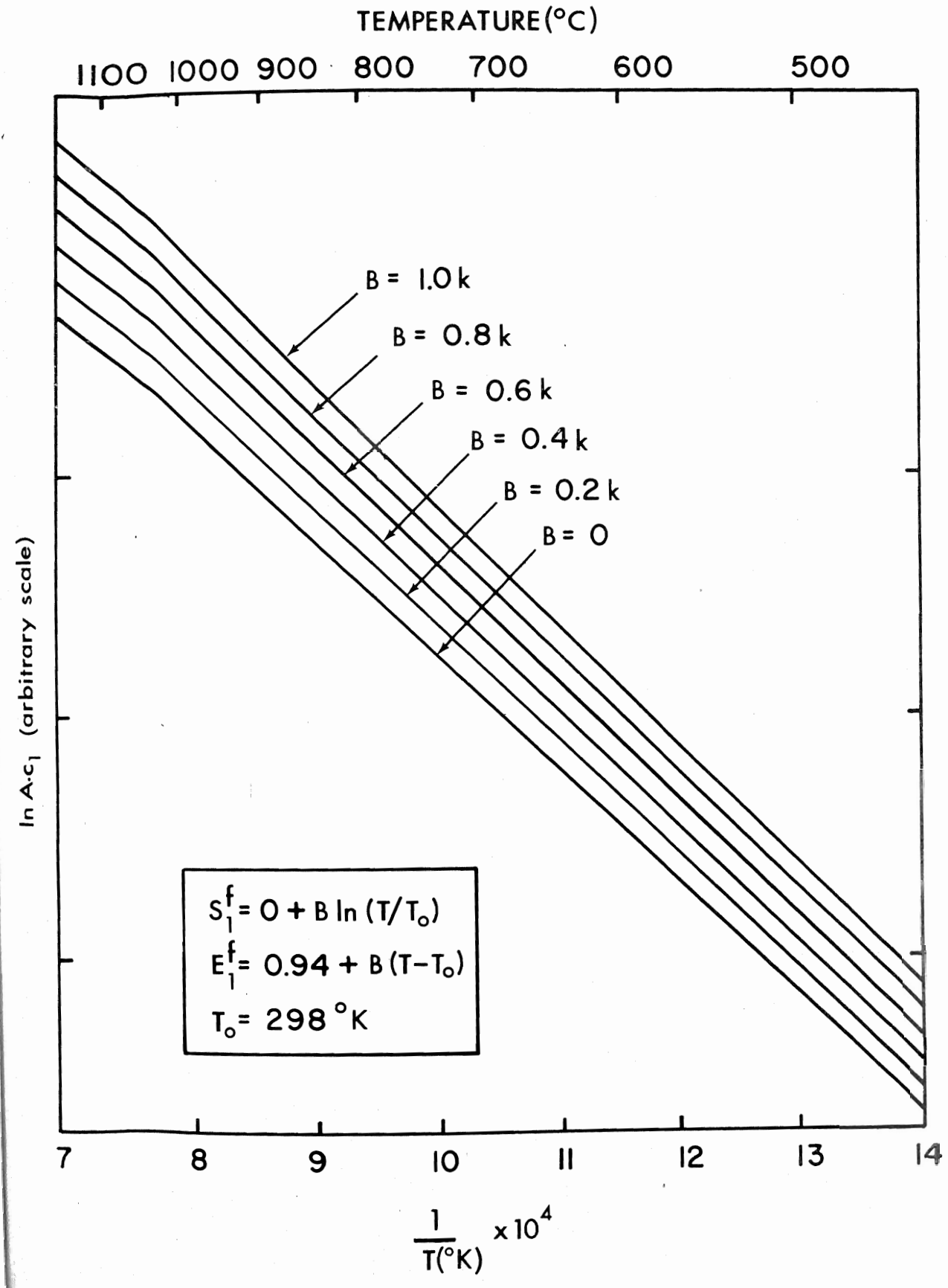
TEMPERATURE (°C)
1100 1000 900 800 700 600 500
B = 1.0 k
B = 0.8 k
B = 0.6 k
B = 0.4 k
B = 0.2 k
B = 0
ln A·c1 (arbitrary scale)
S1f = 0 + B ln (T/To)
E1f = 0.94 + B (T−To)
To = 298 °K
7 8 9 10 11 12 13 14
1/T(°K) x 10^4